© 2017. Published by The Company of Biologists Ltd | Development (2017) 144, 3847-3848 doi:10.1242/dev.159715

CORRECTION

Correction: SoxF factors induce Notch1 expression via direct transcriptional regulation during early arterial development. Development doi: 10.1242/dev.146241

Ivy Kim-Ni Chiang[1,*], Martin Fritzsche[2,*], Cathy Pichol-Thievend[1], Alice Neal[2], Kelly Holmes[3], Anne Lagendijk[1], Jeroen Overman[1], Donatella D'Angelo[4], Alice Omini[4], Dorien Hermkens[5], Emmanuelle Lesieur[1], Nicolas Fossat[6], Tania Radziewic[6], Ke Liu[7], Indrika Ratnayaka[2], Monica Corada[8], George Bou-Gharios[7], Patrick P. L. Tam[6,9], Jason Carroll[3], Elisabetta Dejana[8,10], Stefan Schulte-Merker[5], Benjamin M. Hogan[1], Monica Beltrame[4], Sarah De Val[2,‡] and Mathias Francois[1,‡]

[1]Institute for Molecular Bioscience, The University of Queensland, Brisbane, Queensland 4072, Australia. [2]Ludwig Institute for Cancer Research, Nuffield Department of Clinical Medicine, The University of Oxford, Oxford OX3 7DQ, UK. [3]Cancer Research UK, The University of Cambridge, Li Ka Shing Centre, Robinson Way, Cambridge CB2 0RE, UK. [4]Dipartimento di Bioscienze, Universita' degli Studi di Milano, Via Celoria 26, 20133 Milano, Italy. [5]University of Münster, 48149 Münster, Germany Institute for Cardiovascular Organogenesis and Regeneration, Faculty of Medicine, Westfälische Wilhelms-Universität Münster (WWU), Mendelstrasse 7, 48149 Münster and CiM Cluster of Excellence, Germany. [6]Embryology Unit, Children's Medical Research Institute, Westmead NSW 2145, Australia. [7]Institute of Aging and Chronic Disease, University of Liverpool, Liverpool L69 3GA, UK. [8]IFOM, FIRC Institute of Molecular Oncology, 1620139 Milan, Italy. [9]School of Medical Sciences, Sydney Medical School, University of Sydney, Westmead NSW 2145, Australia. [10]Department of Immunology Genetics and Pathology, Uppsala University, 75185 Uppsala, Sweden.

*These authors contributed equally to this work

‡Authors for correspondence (sarah.deval@ludwig.ox.ac.uk; m.francois@imb.uq.edu.au)

There were errors published in 'SoxF factors induce Notch1 expression via direct transcriptional regulation during early arterial development' by Ivy Kim-Ni Chiang, Martin Fritzsche, Cathy Pichol-Thievend, Alice Neal, Kelly Holmes, Anne Lagendijk, Jeroen Overman, Donatella D'Angelo, Alice Omini, Dorien Hermkens, Emmanuelle Lesieur, Ke Liu, Indrika Ratnayaka, Monica Corada, George Bou-Gharios, Jason Carroll, Elisabetta Dejana, Stefan Schulte-Merker, Benjamin Hogan, Monica Beltrame, Sarah De Val and Mathias Francois (2017). *Development* **144**, 2629-2639 (doi: 10.1242/dev.146241).

The contribution of Nicolas Fossat, Tania Radziewic and Patrick P. L. Tam was inadvertently omitted. These authors generated and validated the *Sox7* knockout mouse line used to produce the *Sox7*/*Sox18* double-knockout line (Fig. 9A). An explanation of how this mouse line was generated was absent from the supplementary Materials and Methods. In addition, the middle initial of Benjamin Hogan was missing.

The corrected author list and affiliations appear above. Revised Author contributions and Funding sections, as well as a revised section of the supplementary Materials and Methods that now includes generation of the *Sox7* knockout mouse line, appear below.

The authors apologise to readers for these mistakes.

Author contributions

Conceptualization: I.K.-N.C., M.Frit., S.D.V., M.Fran.; Methodology: I.K.-N.C., M.Frit., S.D.V., M.Fran.; Formal analysis: K.H., J.C.; Investigation: I.K.-N.C., M.Frit., C.P.-T., A.N., K.H., A.L., J.O., D.D., A.O., D.H., E.L., K.L., I.R., M.C., B.M.H.; Resources: A.L., G.B.-G., J.C., S.S.-M., M.B., N.F., T.R., P.P.L.T.; Data curation: K.H., J.C.; Writing - original draft: I.K.-N.C., S.D.V., M.Fran.; Writing - review & editing: I.K.-N.C., B.M.H., M.B., S.D.V., M.Fran.; Visualization: I.K.-N.C., S.D.V., M.Fran.; Supervision: G.B.-G., J.C., E.D., B.M.H., M.B., P.P.L.T., S.D.V., M.Fran.; Project administration: S.D.V., M.Fran.; Funding acquisition: S.D.V., M.B., M.Fran.

Funding

This work was supported by the National Health and Medical Research Council of Australia (NHMRC) (APP1107643); The Cancer Council Queensland (1107631) (M.Fran.); the Australian Research Council Discovery Project (DP140100485, M.Fran.; DP1094008, P.P.L.T.); NHMRC Senior Principal Research Fellowship (APP1003100) (P.P.L.T.); University of Sydney Postdoctoral Fellowship (N.F.); NHMRC Career Development Fellowship (APP1111169) (M.Fran.); the Ludwig Institute for Cancer Research (M.Frit., A.N., I.R., S.D.V.); the Medical Research Council (MR/J007765/1) (K.L., G.B.-G., S.D.V.); the Fondazione Cariplo (2011-0555) (M.B., B.M.H., M.Fran.); and the Biotechnology and Biological Sciences Research Council (BB/L020238/1) (A.N., K.L., G.B.-G., S.D.V.). Deposited in PMC for release after 6 months.

Supplementary Materials and Methods

Generation and analysis of transgenic and mutant mice (final paragraph)

Sox7:tm1 (*Sox7*$^{+/-}$) mice were generated through germline transmission in chimaeras, using VGB6 ES cells (of C57BL/6NTac background) that contained an inactivated *Sox7* allele replaced with a ZEN-Ub1 cassette from Velocigene (*Sox7*$^{tm1(KOMP)Vlcg}$), and

Development (2017) 144, 3847-3848 doi:10.1242/dev.159715

obtained from the KOMP repository at University of California at Davis (https://www.komp.org/pdf.php?projectID=VG10649). Compound *Sox7*$^{-/-}$;*Sox18*$^{-/-}$ mouse embryos were generated on the C57BL/6 background through crossing heterozygous *Sox7*:tm1 to *Sox18*:tm1, generating *Sox7*$^{+/-}$;*Sox18*$^{+/-}$ mice which were subsequently incrossed (Pennisi et al., 2000a). Genotype was confirmed by PCR using the following primers: mSox7(F), TGTAACTTGGAGATCCATAGAGC; mSox7(R), TCATTCTCAGTATTGTTTTGCC; mSox7lacZ(R), TGGATCAGCTAAGCCAGGT; mSox18(F), CCCGACGTCCATCAGACCTC; mSox18(R), GTCGCTTGCGCTCGT-CCTTC; mSox18lacZ(R), CGCCCGTTGCACCACAGATG. All animals used were 7-24 weeks old.

© 2017. Published by The Company of Biologists Ltd | Development (2017) 144, 2629-2639 doi:10.1242/dev.146241

RESEARCH ARTICLE

SoxF factors induce Notch1 expression via direct transcriptional regulation during early arterial development

Ivy Kim-Ni Chiang[1,*], Martin Fritzsche[2,*], Cathy Pichol-Thievend[1], Alice Neal[2], Kelly Holmes[3], Anne Lagendijk[1], Jeroen Overman[1], Donatella D'Angelo[4], Alice Omini[4], Dorien Hermkens[5], Emmanuelle Lesieur[1], Ke Liu[6], Indrika Ratnayaka[2], Monica Corada[7], George Bou-Gharios[6], Jason Carroll[3], Elisabetta Dejana[7,8], Stefan Schulte-Merker[5], Benjamin Hogan[1], Monica Beltrame[4], Sarah De Val[2,‡] and Mathias Francois[1,‡]

ABSTRACT

Arterial specification and differentiation are influenced by a number of regulatory pathways. While it is known that the Vegfa-Notch cascade plays a central role, the transcriptional hierarchy controlling arterial specification has not been fully delineated. To elucidate the direct transcriptional regulators of Notch receptor expression in arterial endothelial cells, we used histone signatures, DNaseI hypersensitivity and ChIP-seq data to identify enhancers for the human *NOTCH1* and zebrafish *notch1b* genes. These enhancers were able to direct arterial endothelial cell-restricted expression in transgenic models. Genetic disruption of SoxF binding sites established a clear requirement for members of this group of transcription factors (SOX7, SOX17 and SOX18) to drive the activity of these enhancers *in vivo*. Endogenous deletion of the *notch1b* enhancer led to a significant loss of arterial connections to the dorsal aorta in Notch pathway-deficient zebrafish. Loss of SoxF function revealed that these factors are necessary for *NOTCH1* and *notch1b* enhancer activity and for correct endogenous transcription of these genes. These findings position SoxF transcription factors directly upstream of Notch receptor expression during the acquisition of arterial identity in vertebrates.

KEY WORDS: Notch1, SoxF, Artery, Arterial enhancer, Endothelial cell, Transcriptional regulation, Zebrafish, Human, Mouse

INTRODUCTION

Genetic specification of arterial fate has long been attributed to regulation downstream of the Vegfa and Notch pathways. Vegfa signalling is essential for arterial specification in both zebrafish and mammalian models, at least partially by stimulating the expression of components of the Notch pathway, while activation of Notch signalling can rescue defects in Vegfa-deficient zebrafish embryos (Lanahan et al., 2010; Lawson et al., 2002; Liu et al., 2003; Visconti et al., 2002). The Notch receptors Notch1 and Notch4 and the delta-like ligands Dll1, Dll4, Jag1 and Jag2 are expressed in endothelial cells, where they play crucial roles in both arteriogenesis and angiogenesis (Lawson et al., 2002; Liu et al., 2003; Phng and Gerhardt, 2009; Roca and Adams, 2007). Ligand binding to the Notch receptor releases the Notch intracellular domain (NICD), which translocates to the nucleus and forms a transcriptional activation complex with the otherwise repressive DNA-bound Rbpj [CSL, Su(H)] (Bray, 2006). Combined ablation of Notch1 and Notch4, which are both principally expressed in arterial endothelial cells during early vascular remodelling (Chong et al., 2011; Jahnsen et al., 2015), results in severe vascular remodelling defects (Krebs et al., 2000), as does ablation of the Notch downstream effector Rbpj or of Dll4, a Notch ligand specific within the vasculature to arteries (Duarte et al., 2004; Gale et al., 2004; Krebs et al., 2004). However, loss of Notch signalling does not fully recapitulate the arterial defects downstream of Vegfa ablation (Carmeliet et al., 1996; Krebs et al., 2000; Lawson et al., 2002), and the arterially restricted gene expression patterns of components of the Notch pathway do not fully overlap with activated Vegfa (Lawson, 2003), suggesting that additional factors are involved in the regulation of Notch-mediated arterial fate.

The SoxF group of transcription factors (Sox7, Sox17 and Sox18) are expressed in endothelial cells from early in development (Francois et al., 2010). While each SoxF member displays a subtly different endothelial expression pattern, all three factors are expressed early in arterial development (Corada et al., 2013; François et al., 2008; Zhou et al., 2015) and share considerable functional redundancy, complicating interpretation of the consequences of gene disruption (Hosking et al., 2009; Zhou et al., 2015). Combined loss of *sox7* and *sox18* in zebrafish, both by morpholino-based knockdown and genetic mutation, resulted in serious arteriovenous malformations similar to those seen after Notch ablation, suggesting that SoxF factors might genetically interact with the Notch pathway in endothelial cells (Cermenati et al., 2008; Hermkens et al., 2015; Herpers et al., 2008; Lawson et al., 2001). Further evidence was provided in mice, where endothelial-specific ablation of *Sox17* caused arterial differentiation and remodelling defects (Corada et al., 2013), and conditional deletion of SoxF factors in the adult resulted in loss of major vessel identity in the retina (Zhou et al., 2015). Inhibition of Vegfa signalling can significantly impact SoxF expression and activity in both mouse and zebrafish models (Kim et al., 2016; Pendeville et al., 2008; Duong et al., 2014; Pennisi et al., 2000b), suggesting that members of the SoxF family lie downstream of Vegfa. Further, SoxF acts in a positive feed-forward loop to maintain *Flk1*

[1]Institute for Molecular Bioscience, The University of Queensland, Brisbane, Queensland 4072, Australia. [2]Ludwig Institute for Cancer Research, Nuffield Department of Clinical Medicine, The University of Oxford, Oxford OX3 7DQ, UK. [3]Cancer Research UK, The University of Cambridge, Li Ka Shing Centre, Robinson Way, Cambridge CB2 0RE, UK. [4]Dipartimento di Bioscienze, Universita' degli Studi di Milano, Via Celoria 26, 20133 Milano, Italy. [5]University of Münster, 48149 Münster, Germany Institute for Cardiovascular Organogenesis and Regeneration, Faculty of Medicine, Westfälische Wilhelms-Universität Münster (WWU), Mendelstrasse 7, 48149 Münster and CiM Cluster of Excellence, Germany. [6]Institute of Aging and Chronic Disease, University of Liverpool, Liverpool L69 3GA, UK. [7]IFOM, FIRC Institute of Molecular Oncology, 1620139 Milan, Italy. [8]Department of Immunology Genetics and Pathology, Uppsala University, 75185 Uppsala, Sweden.
*These authors contributed equally to this work

‡Authors for correspondence (sarah.deval@ludwig.ox.ac.uk; m.francois@imb.uq.edu.au)

M.F., 0000-0002-9846-6882

Received 28 October 2016; Accepted 7 June 2017

Development (2017) 144, 2629-2639 doi:10.1242/dev.146241

(*Kdr*; *kdrl* in zebrafish) expression (Kim et al., 2016). By contrast, the ablation of Notch signalling in the vasculature does not significantly impact the expression of SoxF (Abdelilah et al., 1996; Corada et al., 2013). Different experimental models have positioned SoxF genes both upstream (Corada et al., 2013) and downstream (Lee et al., 2014) of Notch signalling in endothelial cells, suggesting a complex relationship between these two pathways.

Analysis of the only known enhancers for the Notch pathway, namely the arterial-specific *Dll4*-12 (Sacilotto et al., 2013) and *Dll4*in3 enhancers (Sacilotto et al., 2013; Wythe et al., 2013), has demonstrated a crucial role for SoxF factors in the regulation of expression of the Notch ligand *Dll4* in arteries, in combination with Rbpj/Notch binding and in the presence of Ets factors including Erg (Sacilotto et al., 2013; Wythe et al., 2013). Although this work clearly positioned the SoxF and Notch pathways as crucial regulators of arterial specification, and is supported by analysis placing Sox17 upstream of Notch signalling in mouse models (Corada et al., 2013), ablation of arterial marker expression only occurs after the removal of both SoxF factors and Notch signalling in combination (Sacilotto et al., 2013). Consequently, the precise transcriptional hierarchy of SoxF and Notch has yet to be fully established. Although studies of the Notch receptor genes *Notch1* and *Notch4* also identified SoxF binding motifs within putative promoter sequences (Corada et al., 2013; Lizama et al., 2015), a requirement for these SOX motifs in arterial-specific gene expression of Notch receptors has not been established. In this study, we have identified and characterised arterial-specific enhancers directing *NOTCH1/notch1b* gene expression *in vivo*, and used them to demonstrate a direct requirement for SoxF factors in the transcriptional regulation of Notch receptors during early arterial differentiation, positioning SoxF factors upstream of Notch in the acquisition of arterial cell identity.

RESULTS

Identification of an arterial-specific *NOTCH1* intronic enhancer

Previous studies into the transcriptional regulation of the Notch receptors have not extended to the identification or analysis of gene enhancers (cis-regulatory elements) (Corada et al., 2013; Lizama et al., 2015; Wu et al., 2005). We therefore conducted a detailed *in silico* analysis of the *NOTCH1* locus with the aim of identifying novel, arterial-specific enhancers. This analysis focused on human *NOTCH1* in order to take advantage of the wealth of publicly available information describing chromatin modifications in human endothelial cell lines. Using this information, we were able to pinpoint four regions of DNA rich in endothelial cell-specific H3K4me1 and H3K27ac histone modifications and DNaseI digital genomic footprints, all marks closely associated with enhancer activity (Heintzman and Ren, 2009; Sabo et al., 2004) (Fig. 1A, Fig. S1).

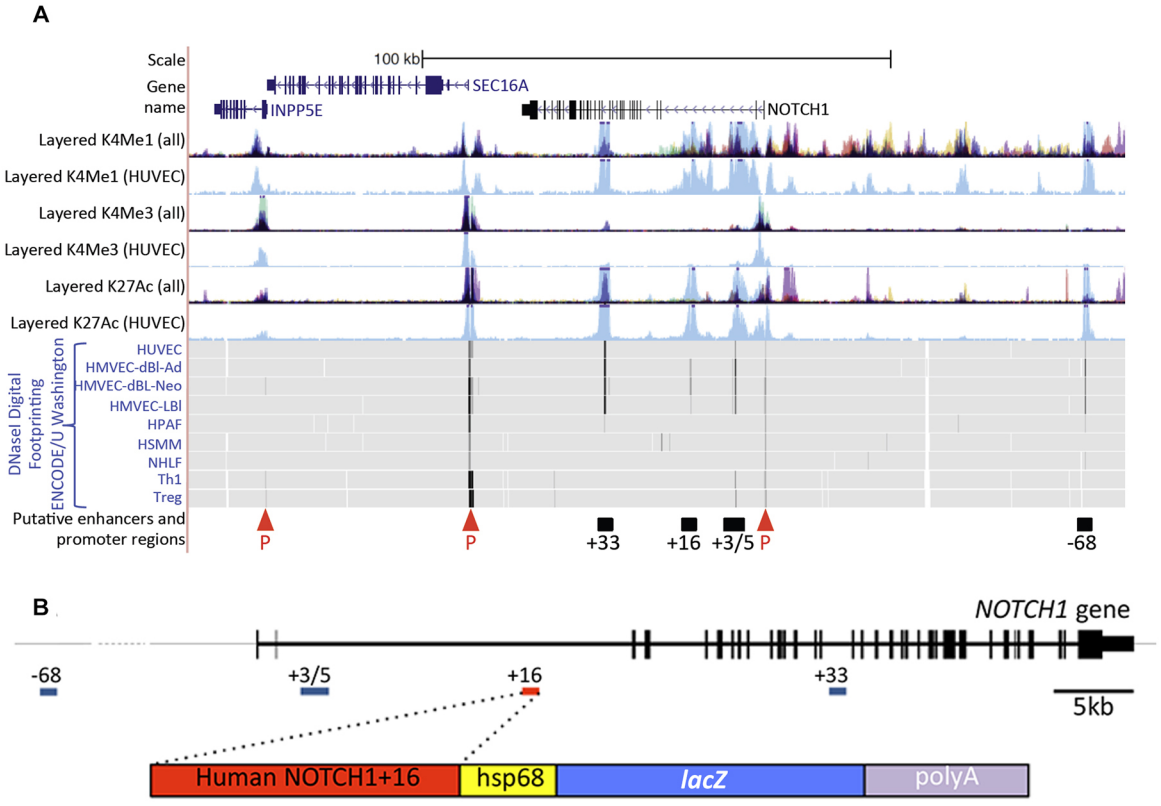

Fig. 1. The human *NOTCH1* locus contains multiple putative endothelial enhancers. (A) The human *NOTCH1* locus from UCSC ENCODE Genome Browser (http://genome.ucsc.edu). Human umbilical vein endothelial cell (HUVEC)-specific H3me1 and H3K27ac (enhancer associated) and H3K4me3 (promoter associated) peaks are indicated in light blue [both in the separate HUVEC and combined tracks (denoted as 'all')]; other colours indicate H3K4me1, H3K4me3 and H3K4ac peaks specific to non-endothelial cell lines: GM12878 cells (red), H1-hESC cells (yellow), HSMM cells (green), K562 cells (purple) NHEK cells (lilac) and NHLF cells (pink). *INPP5E* and *SEC16A* are shown (blue text) in addition to *NOTCH1* (black text). DNase I digital hypersensitive hotspots are indicated by black vertical lines on grey (HUVEC, HMVEC-dBl-Ad, HMVEC-dBl-Neo and HMVEC-LBl, which are all different endothelial cell types). The four *NOTCH1* putative enhancer regions (black bars) were identified by high levels of HUVEC-specific H3K4me1 and H3K27ac associated with endothelial cell-specific DNaseI hypersensitivity hotspots. P, putative promoters identified by H3K4me3. (B) The human *NOTCH1* gene (top, in 5′ to 3′ orientation with putative enhancers indicated) and the *NOTCH1+16hsp* transgene (bottom).

Development (2017) 144, 2629-2639 doi:10.1242/dev.146241

The putative enhancer regions were named *NOTCH1+33*, *NOTCH1+16*, *NOTCH1+3/5* and *NOTCH1−68* to reflect their distance from the transcription start site (TSS) in kb. Each enhancer region was cloned upstream of the silent *hsp68* minimal promoter and the *lacZ* reporter gene (Fig. 1B) and tested for its ability to drive reporter gene expression specifically in arterial endothelial cells of transient transgenic mice at embryonic day (E) 12-13. Although each of the four putative enhancer regions was able to drive detectable levels of *lacZ* in transgenic mice, this expression was primarily neural, an expression pattern commonly seen when using the *hsp68* minimal promoter (e.g. Becker et al., 2016; Sacilotto et al., 2013) (Table 1, Fig. S2). Only the *NOTCH1+33* and *NOTCH1+16* enhancers were able to direct expression in endothelial cells (Table 1, Fig. S2). In the case of *NOTCH1+33*, vascular expression was detected in only one of the five transgenic mice analysed. This expression was not restricted to the arterial endothelium but was pan-endothelial (Table 1, Fig. S2). This agrees with previous reports indicating that the mouse orthologue of this region, termed Notch1_enh1, also directs occasional vascular enhancer activity but did not show arterial-specific expression (Zhou et al., 2017). Conversely, the 274 bp *NOTCH1+16* enhancer was able to robustly direct expression specifically to arterial endothelial cells within the vasculature at E12 in multiple independent transgenic embryos (Table 1, Fig. 2 and Fig. S2). This indicates that the *NOTCH1+16* enhancer represents a novel, arterially restricted enhancer within the *NOTCH1* locus. Analysis of a stable mouse line expressing the *NOTCH1+16:lacZ* transgene clearly demonstrated that this enhancer is strongly active from the very early stages of vascular development, mimicking the expression of endogenous Notch by becoming restricted to the arteries by late E9.5 and then maintaining an arterial endothelial cell-restricted expression pattern throughout embryonic development (Chong et al., 2011; Jahnsen et al., 2015) (Fig. 2).

The *NOTCH1+16* enhancer is bound and regulated by SoxF factors

To identify the transcription factors that potentially regulate the *NOTCH1+16* enhancer, we performed a ClustalW analysis of orthologous mammalian sequences (Fig. 3A). This analysis clearly identified nine conserved core consensus ETS binding motifs [GGAW (Hollenhorst et al., 2011)] and two consensus SOX binding motifs [WWCAAW (Mertin et al., 1999)] (Fig. 3A) within the 274 bp *NOTCH1+16* enhancer. Because not all *in silico* consensus binding motifs are able to functionally bind the cognate protein, these motifs were then tested by electrophoretic mobility shift assay (EMSA). Both SOX motifs (termed hmSOX-a and hmSOX-b) were able to bind recombinant SOX7 and SOX18 proteins in EMSA (Fig. 3B), and three ETS motifs (termed hmETS-a, hmETS-b and hmETS-c) were able to bind the endothelial Ets protein ETV2 (Fig. 3C).

Table 1. Reporter gene expression patterns in E12 mice transgenic for each putative *NOTCH1* enhancer region and the effects of SOX motif mutation on *NOTCH1+16* enhancer activity

Transgene	*n*	Any *lacZ* expression	*lacZ* in AECs	*lacZ* in VECs
NOTCH1−68	5	3	0	0
NOTCH1+3/5	4	4	0	0
NOTCH1+16	10	9	6	0
NOTCH1+33	5	5	1	1
NOTCH1+16 WT	8	7	4	0
NOTCH1+16mutSOX-a/b	9	6	0*	0*

*Faint vascular expression was detected in section analysis but was not visible in whole-mount analysis. *n*, number of transgenic mice analysed. AECs, arterial endothelial cells; VECs, venous endothelial cells.

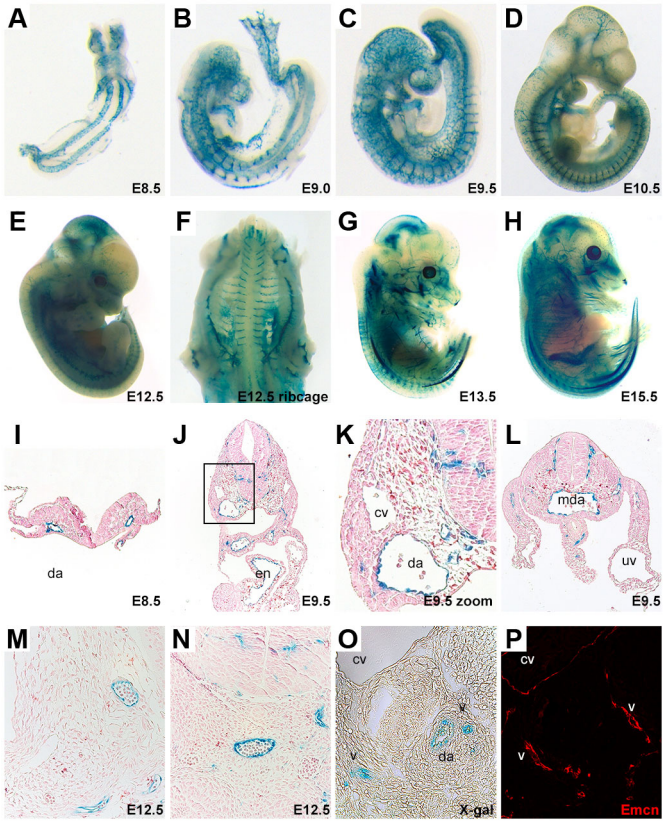

Fig. 2. The *NOTCH1+16* transgene directs arterial endothelial cell-restricted expression in transgenic mice. (A-N) Representative transgenic whole-mount embryos (A-H) and transverse sections (I-N) showing *lacZ* reporter gene expression (β-galactosidase detected by blue X-gal staining) in arterial endothelial cells throughout embryonic development. The boxed region in J is magnified in K. (O,P) E12 transverse section showing that expression of the venous marker endomucin (Emcn) does not overlap with *lacZ* reporter gene expression on the same section. cv, cardinal vein; da, dorsal aorta; Emcn, endomucin; en, endocardium; mda, midline dorsal aorta; uv,umbilical vein; v, vein.

ETS motifs are common to all endothelial-expressed gene enhancers (De Val and Black, 2009). Although the Ets factor Erg has been implicated in arterial specification (Wythe et al., 2013), previous studies have shown that ETS motifs were unable to direct expression of the arterial-specific *Dll4* and *Flk1* enhancers without additional transcription factor binding motifs (Becker et al., 2016; Sacilotto et al., 2013; Wythe et al., 2013), suggesting that Ets factors alone are unlikely to regulate the *NOTCH1+16* enhancer.

To test whether the SOX motifs play a role in *NOTCH1+16* enhancer activity, we mutated the core nucleotides of these motifs (see Materials and Methods for sequences) and tested the ability of the resultant *NOTCH1+16mutSOX-a/b* enhancer to drive reporter gene expression. Strikingly, enhancer mutation resulted in a dramatic reduction in reporter gene expression in endothelial cells in transgenic mice, although transgene expression was detected outside of the vascular system (Fig. 4, Table 1). This result differs notably from that reported for the *Dll4* enhancers, where mutations in SOX motifs, or loss of SoxF factors, resulted in no detectable decrease in *Dll4* expression unless accompanied by ablation of Notch signalling (Sacilotto et al., 2013).

Development (2017) 144, 2629-2639 doi:10.1242/dev.146241

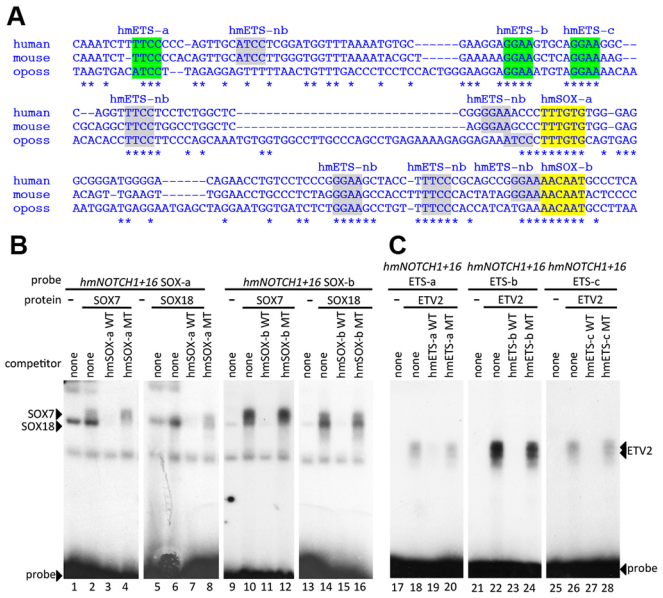

Fig. 3. The *NOTCH1+16* enhancer contains SOX and ETS binding motifs. (A) Multispecies alignment of the orthologous region of the *NOTCH1+16* enhancer from human, mouse and opossum (oposs) using ClustalW. Coloured sequences are confirmed by EMSA; grey sequences are motifs identified *in silico* that did not bind in EMSA. (B) Radiolabelled oligonucleotide probes encompassing *NOTCH1+16* hmSOX-a (lanes 1-8) and hmSOX-b (lanes 9-16) were bound to recombinant SOX7 (lanes 2-4 and 10-12) and SOX18 (lanes 6-8 and 14-16). Both proteins, which efficiently bound labelled probes (lanes 2, 6, 10 and 14), were competed by excess unlabelled self-probe (WT, lanes 3, 7, 11 and 15) but not by mutant self-probe (MT, lanes 4, 8, 12 and 16). (C) Radiolabelled oligonucleotide probes encompassing *NOTCH1+16* hmETS-a (lanes 17-20), hmETS-b (lanes 21-24) and hmETS-c (lanes 25-28) were bound to recombinant ETV2 protein. ETV2, which efficiently bound to labelled probes (lanes 18, 22 and 26), was competed by excess unlabelled self-probe (WT, lanes 19, 23 and 27) but not by mutant self-probe (MT, lanes 20, 24 and 28).

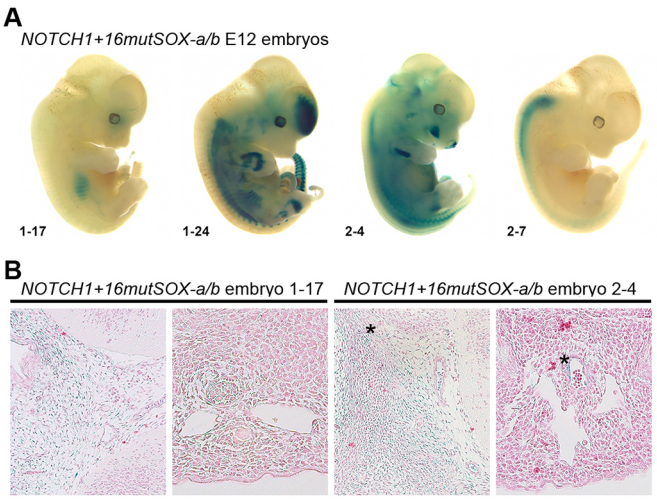

Fig. 4. SoxF factors are required for *NOTCH1+16* activity. (A) Four representative whole-mount E12 X-gal-stained embryos transgenic for the *NOTCH1+16mutSOX-a/b* construct. Numbers at the bottom left indicate the unique embryo identifier. (B) Transverse sections taken from two *NOTCH1+16mutSOX-a/b* embryos demonstrate the very limited endothelial expression detected in these embryos (asterisks). In each case, the section to the left is through the head region, the section to the right is through the upper torso region.

Zebrafish *notch1b* is directly transcriptionally regulated by SoxF factors via an evolutionarily non-conserved enhancer

The SoxF-dependent *NOTCH1+16* enhancer robustly directed arterial-restricted expression in transgenic mouse models. However, this enhancer did not exhibit sequence conservation beyond mammals (Fig. S1B), leaving it unclear how relevant these observations are to Notch signalling during arteriovenous specification in zebrafish, an extremely well-studied model system (Gore et al., 2012). We therefore investigated whether SoxF factors were able to transcriptionally regulate the zebrafish orthologue of *NOTCH1*, *notch1b*, by examining the binding patterns of the zebrafish SoxF transcription factors around the *notch1b* locus. Zebrafish SoxF are expressed in early endothelial cells and implicated in arteriovenous differentiation (Cermenati et al., 2008; Hermkens et al., 2015; Herpers et al., 2008; Pendeville et al., 2008). To probe for SoxF (Sox7, Sox17 and Sox18) genome-wide binding locations we used an endothelial-specific SOX18Ragged overexpression line. The SOX18Ragged dominant-negative protein has been shown to interfere with the endogenous function of all three SoxF transcription factors (James et al., 2003; Pennisi et al., 2000b). Using 26-28 hours post fertilisation (hpf) embryos from the *tg(fli1a:Gal4FF;10×UAS:Sox18Ragged-mCherry)* zebrafish line, in which a tagged SOX18Ragged is expressed specifically in endothelial cells (Fig. S3A), ChIP-seq analysis identified a SoxF binding event 15 kb upstream of the *notch1b* first exon (Fig. 5A). This binding peak was enriched in the enhancer-associated histone modifications H3K4me1 and H3K27ac at 24 hpf (Bogdanović et al., 2012; Kent et al., 2002) (Fig. 5A), suggesting that it might represent a novel enhancer of *notch1b*. A 1219 bp zebrafish DNA fragment corresponding to the SOX18-bound region, termed the *notch1b-15* enhancer, was cloned upstream of a silent *gata2a* promoter and *GFP* reporter gene within the zebrafish enhancer detection (ZED) vector (Bessa et al., 2009) (Fig. 5B) and used to generate the stable *tg(notch1b-15:GFP)* fish line (Fig. 5C). The *GFP* transcript was detected in the vascular cord around the midline from 19 hpf, and persisted in the vascular rod as it formed the dorsal aorta at 22 hpf (Fig. 5C). GFP expression continued to be restricted to the dorsal aorta and the segmental arteries in larvae from 24 hpf until 48 hpf. This arterial-restricted pattern of expression within the vasculature was similar to that of endogenous *notch1b* (Fig. S3B), indicating that the SOX18-bound *notch1b-15* element is a bona fide *notch1b* enhancer and suggesting that SoxF factors directly transactivate Notch receptor transcription in arterial endothelial cells in zebrafish.

ClustalW analysis comparing the orthologous enhancer sequences from fugu, stickleback and medaka revealed a remarkably similar pattern of conserved transcription factor motifs when compared with the *NOTCH1+16* enhancer (Fig. 6A), with multiple ETS and two SOX binding motifs, termed zfSOX-a and zfSOX-b, confirmed by EMSA analysis (Fig. 6B,C). To establish whether the zfSOX-a and zfSOX-b binding motifs were required for *notch1b-15* arterial enhancer function, we generated transient transgenic fish lines harbouring mutated SOX binding motifs (*notch1b-15mutSOX-a/b:GFP*) and compared the activity of the transgene with wild-type (WT) *notch1b-15:GFP* control transient transgenic animals (Fig. S4A,B). Simultaneous disruption of both zfSOX-a and zfSOX-b sites led to a reduction of arterial-specific GFP expression in endothelial cells. Although a minority of mutant fish still expressed GFP after SOX binding site mutation, the loss of expression was still much greater than that seen after SOX motif mutation in a previously published *Dll4* enhancer in transgenic zebrafish, where vascular expression rates were unaffected by

Development (2017) 144, 2629-2639 doi:10.1242/dev.146241

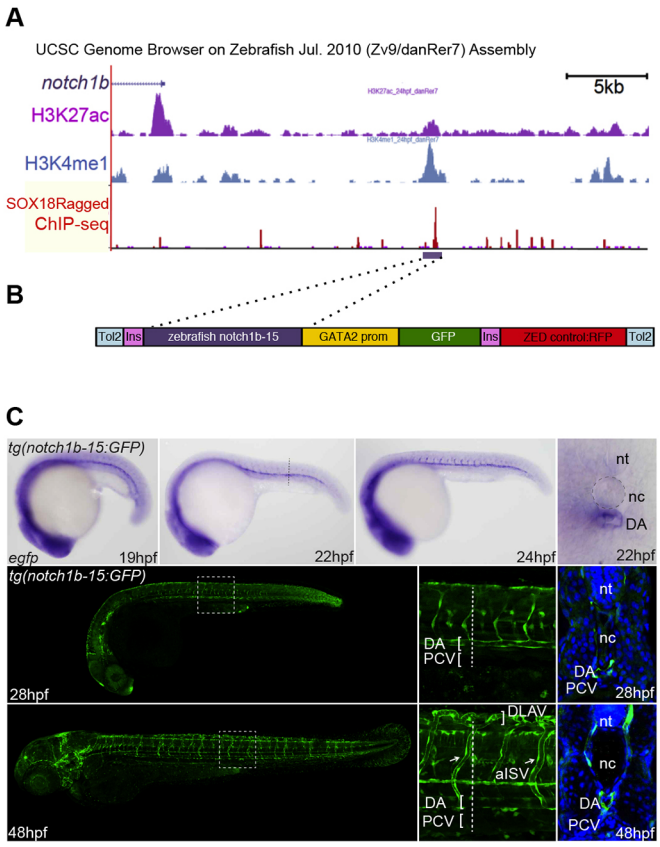

Fig. 5. A SOX18-bound region within the *notch1b* locus represents a bona fide arterial-specific enhancer. (A) Part of the zebrafish *notch1b* locus from the UCSC ENCODE Genome Browser. The *notch1b* gene is in 3′ to 5′ orientation, H3K27ac peaks at 24 hpf are in purple, H3K4me1 peaks at 24 hpf are blue, SOX18Ragged ChIP-seq peaks are red, and the region encompassing the *notch1b-15* enhancer is indicated by the purple horizontal bar. (B) The ZED *notch1b-15:GFP* transgene. Ins, insulator sequences; GATA2 prom, the silent *GATA2* promoter; ZED control:RFP, the active cardiac actin enhancer/promoter construct fused to the *RFP* gene used as a positive control in the ZED vector. (C) The *notch1b-15:GFP* transgene directs arterial endothelial cell-specific expression in the zebrafish line *tg(notch1b-15:GFP)*. Representative transgenic whole-mount embryos and transverse sections show reporter gene expression, as detected by *in situ* hybridisation (top row, blue) or GFP fluorescence (bottom rows, green) in arterial endothelial cells throughout embryonic development. nt, neural tube; nc, notochord; DA, dorsal aorta; PCV, posterior cardinal vein; aISV (arrows), arterial intersomitic vessel; DLAV, dorsal longitudinal anastomotic vessel.

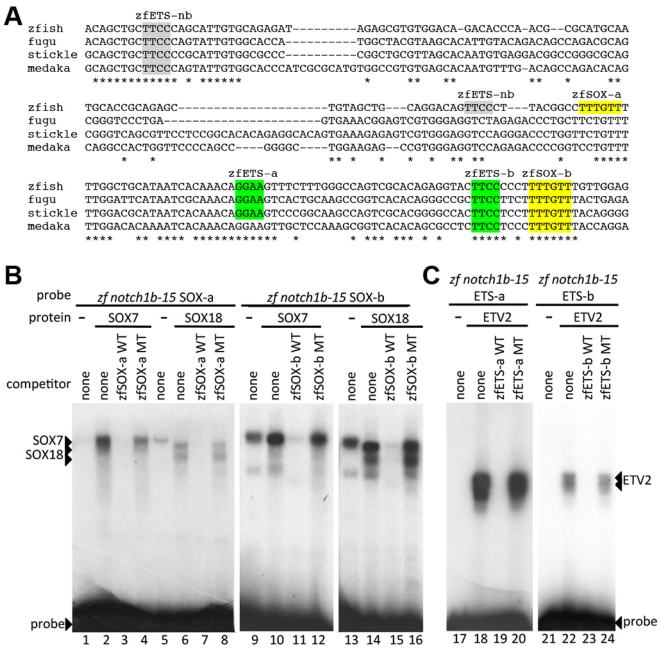

Fig. 6. The *notch1b-15* enhancer contains essential SoxF binding motifs. (A) Multispecies alignment of the orthologous regions of the *notch1b-15* enhancer from zebrafish (zfish), fugu, stickleback (stickle) and medaka using ClustalW. Coloured sequences are confirmed by EMSA; grey sequences are motifs identified *in silico* that did not bind robustly in EMSA. (B) Radiolabelled oligonucleotide probes encompassing *notch1b-15* zfSOX-a (lanes 1-8) and zfSOX-b (lanes 9-16) were bound by recombinant SOX7 (lanes 2-4 and 10-12) and SOX18 (lanes 6-8 and 14-16). Both proteins, which efficiently bound labelled probes (lanes 2, 6, 10 and 14), were competed by excess unlabelled self-probe (WT, lanes 3, 7, 11 and 15) but not by mutant self-probe (MT, lanes 4, 8, 12 and 16). (C) Radiolabelled oligonucleotide probes encompassing *notch1b-15* zfETS-a (lanes 17-20) and zfETS-b (lanes 21-24) (see A) were bound by recombinant ETV2 proteins. ETV2, which efficiently bound to labelled probes (lanes 18 and 22), was competed by excess unlabelled self-probe (WT, lanes 19 and 23) but not by mutant self-probe (MT, lanes 20 and 24).

mutations of SoxF binding motifs (Sacilotto et al., 2013), supporting a key role for SoxF factors in *notch1b* activation. To further confirm our observation, we established stable transgenic *notch1b-15mutSOX-a/b:GFP* fish lines and compared them with the established WT *notch1b-15:GFP* lines. Analysis of the stably transgenic embryos (Fig. 7A) confirmed a GFP expression pattern in the dorsal aorta and segmental arteries for the WT transgene. By contrast, the *tg(notch1b-15mutSOX-a/b:GFP)* lines showed ectopic GFP expression in neurons and a significant decrease of GFP expression in the arterial endothelium (Fig. 7A). Quantitative analysis of GFP intensity in both dorsal aorta and segmental arteries showed lower expression in most *tg(notch1b-15mutSOX-a/b:GFP)* than in WT *tg(notch1b-15:GFP)* embryos (Fig. 7B,C, Fig. S4C). Taken together, these data clearly demonstrate that the zfSOX-a/b binding sites are required to guide *notch1b-15*-specific enhancer activity *in vivo* during arterial development.

We next investigated the consequences of morpholino (MO)-based knockdown of SoxF on *tg(notch1b-15:GFP)* fish. *sox7/sox18* double morphants exhibit a severe vascular phenotype (Fig. S5), including fusions and shunts between the dorsal aorta and cardinal vein (Cermenati et al., 2008; Herpers et al., 2008; Pendeville et al., 2008), phenotypes that are shared with *sox7;sox18* double-mutant fish (Hermkens et al., 2015). MO-induced transcript depletion of *sox7* or *sox18* resulted in downregulation of *notch1b-15:GFP* expression, while *sox7/sox18* double-morphant *tg(notch1b-15:GFP)* fish demonstrated a near-complete loss of reporter gene expression (Fig. 7D,E).

Taken together, these results indicate that SoxF proteins directly modulate the activity of arterial-specific enhancers for both the mammalian NOTCH1 and zebrafish Notch1b receptors, positioning SoxF transcription factors directly upstream of Notch signalling during early arterial differentiation in both mammals and zebrafish.

Loss of endogenous *notch1b-15* enhancer activity perturbs *notch1b* transcription and causes arteriovenous defects

To assess whether the endogenous *notch1b-15* regulatory element is functionally relevant during arteriovenous differentiation *in vivo*, we deleted the endogenous *notch1b-15* enhancer in zebrafish. The resultant *notch1b-15*^{uq1mf} allele was generated using two guide RNAs to drive rapid genome editing using the CRISPR/Cas9 system (Fig. 8A), resulting in excision of a 203 bp fragment overlapping the

Development (2017) 144, 2629-2639 doi:10.1242/dev.146241

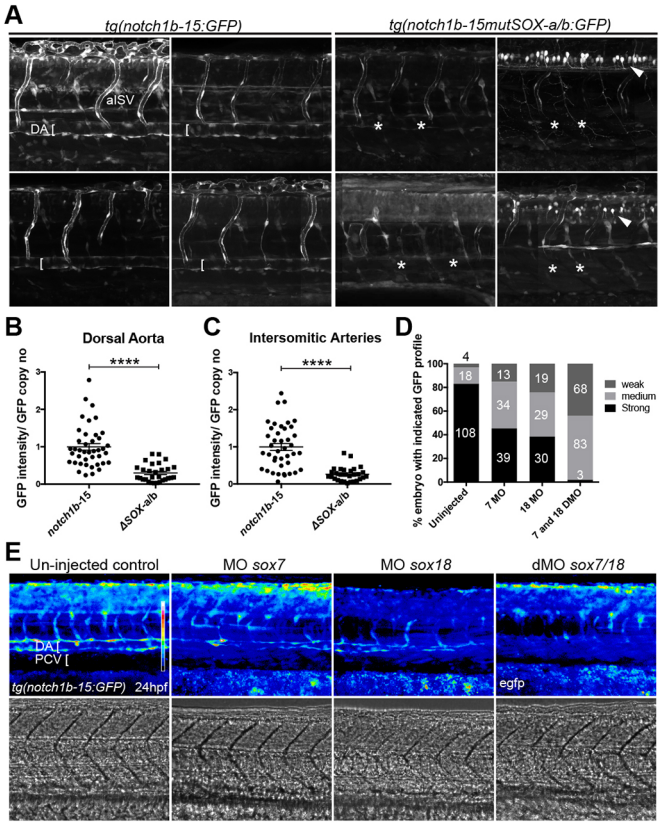

Fig. 7. SoxF factors are required for *notch1b-15* activity. (A) Confocal projection of stably transgenic WT *tg(notch1b-15:GFP)* (left) and *tg(notch1b-15mutSOX-a/b:GFP)* (right), where both zfSOX-a and zfSOX-b sites have been simultaneously mutated. Representative larvae from four independent founders are shown. Asterisks indicate the reduced GFP expression in the dorsal aorta. Arrowheads show the ectopic neuronal expression observed in *tg(notch1b-15mutSOX-a/b:GFP)*. All panels show composite images from tile scan acquisition. (B,C) The intensity of GFP expression in the dorsal aorta and arterial intersomitic vessels of the stably transgenic *tg(notch1b-15:GFP)* and *tg(notch1b-15mutSOX-a/b:GFP)* at 2 dpf. Expression is normalised to *GFP* genomic copy number. Fish were pooled from three or four separate founders. Mean±s.e.m. *tg(notch1b-15)*, *n*=41; *tg(notch1b-15mutSOX-a/b:GFP)*, *n*=29. ****P<0.0001 (Mann–Whitney *U*-test). (D) Levels of GFP expression in *tg(notch1b-15:GFP)* zebrafish embryos after MO injection. Number of fish for each condition is indicated. (E) Representative examples of *sox7/18* double-morphant *tg(notch1b-15:GFP)* zebrafish at 24 hpf as compared with uninjected controls. Double morphants (dMO) demonstrated reduced EGFP expression in the dorsal aorta and intersomitic vessels. DA, dorsal aorta; PCV, posterior cardinal vein; aISV, arterial intersomitic vessel.

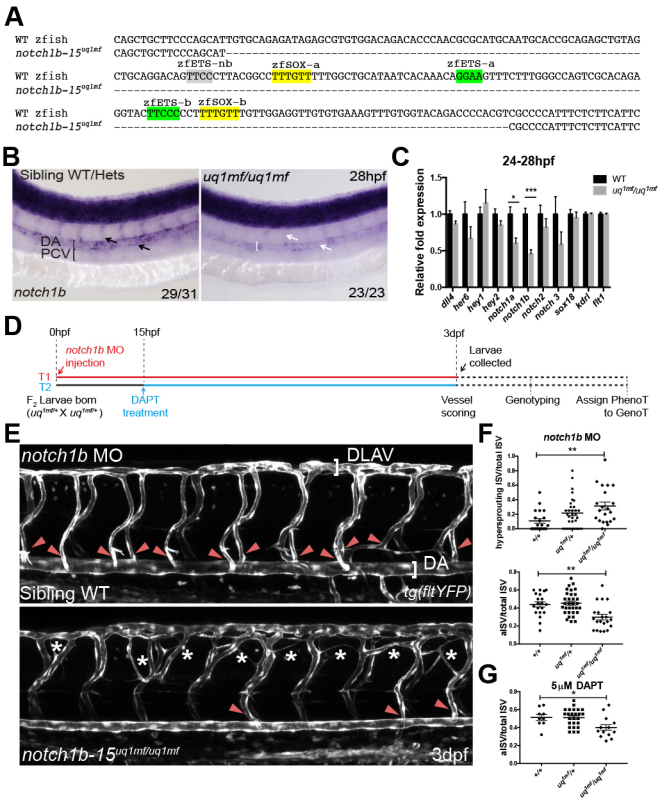

Fig. 8. Loss of endogenous *notch1b-15* compromises artery formation and reduces the endogenous *notch1b* transcript level. (A) The deleted region (dashed line) of *notch1b-15* mutant allele *uq1mf*, which includes both the zfSOX-a and zfSOX-b sites (yellow). (B) F_2 *notch1b-15*$^{uq1mf/uq1mf}$ has reduced *notch1b* expression in dorsal aorta and intersomitic vessels (white arrows) as compared with sibling WT and heterozygotes (black arrows) at 26-28 hpf. The number of embryos showing the illustrated phenotype among the total examined is indicated. (C) Quantitative PCR on FACS-sorted endothelial populations at 24-28 hpf, showing that F_3 *notch1b-15*$^{uq1mf/uq1mf}$ fish have lower *notch1b* expression than WT fish. Expression is relative to *kdrl* and *flt1*. Mean± s.e.m. *n*=6 (*uq1mf/uq1mf*) and *n*=8 (WT) independent sorts, where each sort was pooled from 60-100 larvae;. *P<0.05, ***P<0.001 (*t*-test). (D) The treatment regime conducted to characterise the vascular phenotype of the *uq1mf/+* cross. In treatment 1 (T1, red), *notch1b* MO was injected at the 1-2 cell stage. The developing vasculature of each embryo was then analysed blindly at 3 dpf. After scoring, genotypes were assigned to each larva. In treatment 2 (T2, blue), larvae from the *uq1mf/+* cross were treated with or without DAPT (5 µM) from 15-16 hpf until 3 dpf. Vessels of these treated larvae were blindly scored prior to genotyping, as reported for T1. (E) At 3 dpf, *notch1b-15*$^{uq1mf/uq1mf}$ *notch1b* morphants frequently showed ectopic sprouting in between the intersomitic vessels (asterisks) as compared with sibling WT *notch1b* morphants. Mutants also show loss of arterial connections (red arrowheads) between the dorsal longitudinal anastomotic vessel (DLAV) and dorsal aorta (DA), as indicated by the loss of YFP expression in the *tg(flt1:YFP)* background. (F) (Top) Quantification of hypersprouting ISV number in individual *notch1b* morphants labelled by *tg(flt1:YFP)* at 3 dpf. Mean±s.e.m. Sibling WT (+/+), *n*=20; heterozygote (*uq1mf/+*), *n*=32; homozygous mutant (*uq1mf/uq1mf*), *n*=21. (Bottom) Quantification of YFP-positive intersomitic vessels that connect between DLAV and DA in individual *notch1b* morphants labelled by *tg(flt1:YFP)* at 3 dpf. Mean±s.e.m. Sibling WT, *n*=20; heterozygote, *n*=32; homozygous mutant, *n*=21. **P<0.005 (Mann–Whitney *U*-test). (G) Quantification of YFP-positive intersomitic vessels that connect between DLAV and DA in individual embryos treated with 5 µM DAPT at 3 dpf. Vessels are labelled by *tg(flt1:YFP)*. Mean±s.e.m. Sibling WT, *n*=9; heterozygote, *n*=25; homozygous mutant, *n*=14. *P<0.05 (Mann–Whitney *U*-test).

notch1b-15 enhancer. Analysis of endogenous *notch1b* expression in the F_2 generation demonstrated lower *notch1b* expression levels in both dorsal aorta and arterial intersomitic vessel (aISV) of the *notch1b-15*$^{uq1mf/uq1mf}$ homozygous embryos as compared with their sibling controls, whereas no change was observed in the neural tube (Fig. 8B). Next, we assessed the *notch1b* transcript levels in purified *flt1*-positive arterial endothelial cell populations from the F_3 generation of homozygous fish (F_2 *notch1b-15*^{uq1mf} homozygous in-cross) compared with WT control larvae (F_2 *notch1b-15*$^{+/+}$ × *flt1:YFP;lyve1:dsRed*) at 24-28 hpf (Fig. 8C). As expected, *notch1b* transcripts were significantly downregulated in the homozygous animals, strongly supporting a role for the *notch1b-15* enhancer in the transcription of endogenous *notch1b* in arterial endothelial cells.

To assess the phenotypic outcome of *notch1b-15* loss of function, we took advantage of the *tg(notch1b-15*$^{uq1mf/+}$*;flt1:YFP;lyve1:dsRed)* line to analyse the developing vasculature after *notch1b-15* enhancer deletion in both the F_2 and F_3 generations. Surprisingly, given the reduced levels of *notch1b* (Fig. 8B), no overt vascular

Development (2017) 144, 2629-2639 doi:10.1242/dev.146241

phenotype was detected in F_2 *notch1b-15*$^{uq1mf/uq1mf}$ homozygous zebrafish (F_1 heterozygous *notch1b-15*$^{uq1mf/+}$ in-cross) (Fig. S6A), suggesting partial enhancer redundancy. Such redundancy, which is potentially explained by the pervasiveness of redundant, or 'shadow', enhancers around developmental genes (Cannavò et al., 2016), has previously been well documented in key endothelial genes, with examples including the *Dll4*, *Flk1* and *Tal1* loci (Cannavò et al., 2016). By contrast, we detected a subpopulation (20-30%) of larvae from the F_3 generation (F_2 homozygous *notch1b-15*$^{uq1mf/uq1mf}$ in-cross) that displayed a phenocopy of the *notch1b* loss-of-function phenotype (Fig. S6B). This increase in the phenotypic severity in the F_3 generation suggests that, in the context of the *notch1b-15*$^{uq1mf/+}$ cross, maternal mRNA deposition is likely to help compensate for the disruption of *notch1b* transcription caused by deletion of the *notch1b* enhancer, a compensation that is reduced in a purer *notch1b-15*$^{uq1mf/uq1mf}$ genetic background (Harvey et al., 2013).

To bypass potential rescue effects of shadow enhancers or maternally deposited transcripts, we also investigated arteriovenous differentiation and sprouting angiogenesis in F_2 *notch1b-15*$^{uq1mf/uq1mf}$ zebrafish after low-level depletion of *notch1b* mRNA. A splice *notch1b* MO was injected into eggs from a *notch1b-15*$^{uq1mf/+}$ in-cross in the *tg(flt1:YFP;lyve1:dsRed)* background. The *notch1b* MO was used at suboptimal concentration (5 ng/embryo), which is known to result in minimal phenotypes (Sacilotto et al., 2013). The developing vasculature of each resulting embryo was analysed blindly at 3 dpf, and genotypes were assigned to embryos after image acquisition (Fig. 8D, red). Whereas most WT siblings had normal ISV development, we observed an increased number of hypersprouting ISVs across the *notch1b-15*$^{uq1mf/+}$ and *notch1b-15*$^{uq1mf/uq1mf}$ population (Fig. 8E, asterisks; Fig. 8F, top) in a gene dosage-dependent manner, similar to the phenotype described previously in high MO concentration *notch1b* morphants and Notch signalling-deficient embryos (Geudens et al., 2010; Siekmann and Lawson, 2007). Further, mutant embryos also demonstrated loss of arterial connections between the dorsal aorta and dorsal longitudinal anastomotic vessel, similar to those described in Notch signalling-deficient zebrafish (Geudens et al., 2010; Quillien et al., 2014), while the *notch1b*-depleted *notch1b-15*$^{+/+}$ and *notch1b-15*$^{uq1mf/+}$ morphant embryos demonstrated an equal proportion of arterial and venous ISVs as previously reported (Bussmann et al., 2010) (Fig. 8E,F bottom).

To further confirm that interfering with *notch1b-15* enhancer activity is additive to *notch1b* transcript depletion, we chemically treated the *notch1b-15*$^{uq1mf/+}$ cross with DAPT, a well characterised Notch signalling inhibitor, over the course of endothelial differentiation (15- to 16-somite stage through to 3 dpf) (Fig. 8D, blue). All embryos treated with a suboptimal concentration of DAPT (5 µM) showed a straight body axis, indicating that somitogenesis (and therefore Notch activity) was not significantly compromised (Fig. S7A). Interestingly, despite this lack of morphological defects, F_2 fish homozygous for the *notch1b-15*^{uq1mf} allele displayed a lower arterial-to-total ISV ratio (Fig. 8G, Fig. S7A). By contrast, fish homozygous for the *notch1b-15*^{uq1mf} allele treated with DMSO vehicle alone had a comparable aISV ratio to both *notch1b-15*$^{+/+}$ and *notch1b-15*$^{uq1mf/+}$ siblings (Fig. S7B), similar to the untreated control. This suggests that the observed loss of aISV is specific to an additive effect of DAPT treatment and *notch1b-15* enhancer activity disruption. Overall, these data suggest a functional role of the *notch1-15* enhancer in the endothelial-specific initiation of *notch1b* transcription to promote the acquisition of arterial cell identity.

SoxF factors are required for endogenous *Notch1*/*notch1b* expression

Our results have clearly implicated SoxF factors as direct upstream regulators of arterial Notch enhancers, and therefore suggest a considerably greater role for SoxF in the regulation of the Notch receptors than of the Notch ligands. However, since the *notch1b-15* enhancer is partially redundant with other *notch1b* shadow enhancers, we wished to establish whether SoxF regulation is required for endogenous *notch1b* expression itself, not just enhancer activity. Further, our results so far do not entirely rule out the possibility of SoxF/Rbpj combinatorial regulation of *notch1b*, as was previously shown for *Dll4* enhancers (Sacilotto et al., 2013). Although neither the human *NOTCH1+16* nor the zebrafish *notch1b-15* enhancer contains conserved consensus Rbpj/Notch binding motifs, transcription factors can bind non-consensus motifs, and not all transcription factors necessarily bind conserved motifs (Wong et al., 2015). The nature of the SoxF/Notch combinatorial regulation of *Dll4*, where the SOX or RBPJ binding motifs play functionally interchangeable roles, indicates potential direct interactions between these two proteins, such that only a single SOX binding motif might be necessary for SoxF/Rbpj synergy. We therefore investigated the consequences of SoxF depletion on endogenous *Notch1*/*notch1b* expression *in vivo*.

Although *Sox17* is robustly expressed in arterial endothelial cells (Corada et al., 2013; Hosking et al., 2009), compound *Sox7;Sox18* deletion in mice resulted in a reduction of *Notch1* mRNA levels in the trunk dorsal aorta and primitive heart cavities of E8.5 embryos (Fig. 9A, Fig. S8A). These results concur with observations in the mouse retina, where the vascular phenotype after *Sox7;Sox17;Sox18* endothelial-specific triple deletion closely resembled defects caused by loss of Notch signalling (Zhou et al., 2015). Strikingly, both MO-induced gene knockdown and compound mutation of *sox7* and *sox18* in zebrafish embryos also led to a near-complete loss of *notch1b* transcript expression specifically in endothelial cells, as shown by *in situ* hybridisation analysis (Fig. 9B,C, Fig. S8B). These results further establish an essential role for SoxF transcription factors in the induction of *Notch1*/*notch1b* gene expression, and position SoxF proteins at the top of the transcriptional hierarchy regulating arterial specification.

DISCUSSION

Recent work has implicated SoxF, Ets and Rbpj, the Notch transcriptional effector, in the regulation of the Notch ligand *Dll4* and many other key arterial genes (Corada et al., 2013; Lizama et al., 2015; Sacilotto et al., 2013; Wythe et al., 2013), but has not established the hierarchical arrangement of these diverse factors in arterial specification and differentiation. In this study, we demonstrate that arterial expression of the Notch receptor *Notch1*/*notch1b*, a key player in arterial specification, is directly downstream of SoxF regulation in both fish and mouse. Unlike other key arterial specification markers, including Dll4, Efnb2a and Dlc (Sacilotto et al., 2013), ablation of Notch1/Notch1b expression after depletion of SoxF factors occurred without concurrent inhibition of Notch signalling. Therefore, this work positions SoxF factors directly above Notch signalling in the transcriptional hierarchy initiating arterial development, and suggests that SoxF factors might initiate a feed-forward loop directing arterial identity. In this model, SoxF factors would first activate Notch signalling via the transcriptional activation of Notch receptors in combination with weak activation of Notch ligands (Sacilotto et al., 2013). This early SoxF-mediated activity would then be boosted by the initiation of Notch signalling, resulting in the sustained activation

Development (2017) 144, 2629-2639 doi:10.1242/dev.146241

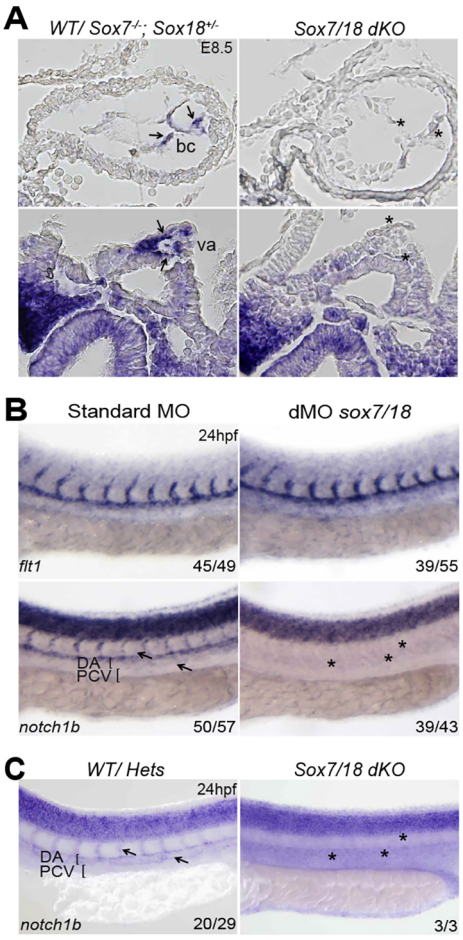

Fig. 9. Mouse and zebrafish arterial *Notch1* expression is dependent on SOX7/18 activity. (A) Transverse sections of whole-mount *in situ* hybridisation for *Notch1* transcript on E8.5 mouse embryos shows a reduction of *Notch1* expression (asterisks) in the bulbus cordis (bc) region of the primitive heart and vitelline artery (va) of *Sox7*/*Sox18* double knockouts. (B) At 24 hpf *notch1b* expression is significantly downregulated in the dorsal aorta (asterisks) of *sox7*/*sox18* double-morphant zebrafish, whereas its signal is unaffected in the neural tube. *flt1* expression is comparable between controls and *sox7*/*sox18* double morphants, indicating that the dorsal aorta is correctly formed. (C) *notch1b* was barely detectable in the dorsal aorta and ISVs of *sox7*/*18* double-knockout zebrafish (asterisks), as compared with the WT, *sox7* or *sox18* heterozygotes (arrows). The number of embryos showing the illustrated phenotype among the total examined is indicated. DA, dorsal aorta; PCV, posterior cardinal vein.

of other downstream genes, eventually activating the full cohort of genes necessary to acquire and maintain arterial endothelial cell identity.

Understanding the function of SoxF factors through mutational analysis has presented significant challenges. Strain-specific variations in mice after depletion of individual SoxF genes and varying levels of compensation from other SoxF factors have resulted in some contradictory reports (Corada et al., 2013; Lee et al., 2014), as is also the case for zebrafish morphant analysis (Cermenati et al., 2008; Herpers et al., 2008; Pendeville et al., 2008). Nonetheless, the results described here agree with an increasingly convincing body of work suggesting that SoxF factors influence Notch signalling yet are unaffected by Notch ablation. For example, overexpression of Sox17 upregulates components of the Notch pathway (Corada et al., 2013; Lizama et al., 2015), loss of functional SoxF factors results in defects similar to those observed after Notch inhibition in mice and fish (Corada et al., 2013; Sakamoto et al., 2007; Zhou et al., 2015), while Notch ablation results in little alteration to the endothelial expression of SoxF factors in mice and fish (Abdelilah et al., 1996; Corada et al., 2013). Data reported here combine with these reports to strongly support a role for SoxF factors as part of the initial transcriptional machinery that instructs arterial specification events.

However, some questions remain. In particular, it is notable that *sox7;sox18* double-mutant fish, although exhibiting severe arteriovenous defects very similar to those seen in Notch-deficient fish (Lawson et al., 2001), do not fully recapitulate the effects of Vegfa depletion on arterial specification (Lawson et al., 2002). While this difference may in part be attributed to weak expression of zebrafish *sox17*, which is expressed in some arterial endothelial cells (Hermkens et al., 2015), it is also expected that the Vegfa pathway has a wider effect on arterial endothelial cells more generally, away from SoxF-mediated activation of Notch signalling. SoxF factors are also influenced by signalling pathways beyond Vegfa. The diverse nature of Vegfa roles in the vasculature, including the regulation of both sprouting angiogenesis and arteriogenesis, processes that inevitably involve different cohorts of downstream targets, make it necessary that multiple regulatory pathways interact with Vegfa during vascular development. While recent work has shown that Vegfa signalling increases the nuclear translocation of SoxF (Duong et al., 2014), and inhibition of Vegfa results in the loss of vascular *sox7* in fish, *sox18* is still expressed in the absence of intact Vegfa signalling (Pendeville et al., 2008). Additionally, loss of the Vegf co-receptor Nrp1 has little effect on SoxF expression in mouse retinal vasculature (Zhou et al., 2015), pointing to other upstream influences on SoxF function in endothelial cells. Other upstream effectors of SoxF function are likely to include canonical Wnt signalling and Vegfd, both of which have been shown to influence SoxF nuclear localisation (Corada et al., 2013; Duong et al., 2014; Zhou et al., 2015).

Recent evidence has also implicated a role for a coordinated Vegf-Mapk-Ets pathway in the induction of Notch signalling components and early arterial differentiation (Wythe et al., 2013). Notably, in addition to SoxF motifs, both the *Notch1* and *Dll4* enhancers share a number of highly conserved consensus motifs for the Ets family of transcription factors. While ETS motifs are common to all vascular enhancer elements, including many that are not preferentially expressed in the arterial vasculature (De Val and Black, 2009), the Ets factor Erg has been specifically implicated in arterial-specific regulation of *Dll4* (Wythe et al., 2013). It is therefore likely that Vegfa-mediated activation of Ets factors may contribute to the transcriptional activity of Notch downstream effectors, and thus may influence arterial establishment independently of SoxF factors. However, it is notable that Vegfa-mediated activation of Ets transcription factors alone does not appear to be sufficient for arterial gene expression. *Dll4* enhancers lacking SOX and RBPJ motifs but retaining all ETS motifs were unable to drive any transgene expression (Sacilotto et al., 2013), nor were Notch enhancers lacking SOX motifs (Figs 2-4). Similar results were found in other delineated arterial enhancers, including the *Ece1* upstream enhancer (Robinson et al., 2014) and the *Flk1* intron 10 enhancer, where loss of Rbpj-mediated repression resulted in expansion of enhancer activity into venous cells without alterations to ETS motif binding (Becker et al., 2016). Combined with recent observations demonstrating that Erg also plays a crucial role in venous specification through activation of *Aplnr* (Lathen et al., 2014),

Development (2017) 144, 2629-2639 doi:10.1242/dev.146241

it is therefore likely that the role of Erg, and of other Ets factors, downstream of Vegfa in arterial-restricted gene expression occurs in co-operation with additional essential, arterial-specifying transcription factors. The data presented in this work, combined with the analysis of further arterial enhancers, including those of *Dll4* and *Ece1* (Robinson et al., 2014; Sacilotto et al., 2013; Wythe et al., 2013), increasingly suggest that SoxF may fulfil this role.

MATERIALS AND METHODS

Cloning

The 10×UAS:Sox18Ragged-mCherry plasmid was generated using the full-length mouse *Sox18Ragged* cDNA sequence, tagged with 10×UAS and mCherry and cloned into pDestTol2CG2 (Kwan et al., 2007). *notch1b-15:GFP* WT was generated by cloning a 1219 bp PCR fragment from zebrafish genomic DNA together with *gata2a* promoter and *GFP* reporter gene into the zebrafish enhancer detection (ZED) vector (Bessa et al., 2009). *notch1b-15mutSOX-a/b* was generated by site-directed PCR mutagenesis of the WT construct. The *NOTCH1−68*, *NOTCH1+3/5* and *NOTCH1+33* enhancers were generated by PCR from human genomic DNA, *NOTCH1+16* WT and *NOTCH1+16mutSOX-a/b* enhancers were generated as custom-made, double-stranded linear DNA fragments (GeneArt Strings, Life Technologies). All mammalian fragments were cloned into the *hsp68-lacZ* Gateway vector (provided by N. Ahituv) (De Val et al., 2004). Primers and sequences for DNA fragments are listed in the supplementary Materials and Methods.

Transgenic animals and genome editing

Animal procedures were approved by local ethical review and licensed by the UK Home Office or conformed to institutional guidelines of the University of Queensland Animal Ethics Committee. Transgenic mice were generated by oocyte microinjection and analysed as detailed in the supplementary Materials and Methods (De Val et al., 2004). Compound $Sox7^{-/-};Sox18^{-/-}$ (C57BL/6) mouse embryos were generated on the C57BL/6 background through crossing heterozygous *Sox7:tm1* to *Sox18:tm1* generating $Sox7^{+/-};Sox18^{+/-}$ mice, which were subsequently in-crossed (Pennisi et al., 2000a).

Transgenic zebrafish embryos were generated using the Tol2 system in conjunction with the ZED vector (Bessa et al., 2009). The $sox7^{hu5626};sox18^{hu10320}$ double-homozygous mutant zebrafish have been described previously (Hermkens et al., 2015). The *tg(fli1a:Gal4FF,10×UAS:Sox18Ragged-mCherry)* zebrafish line was generated by crossing *10×UAS:Sox18Ragged-mCherry* with *fli1a:Gal4FF*, *4×UAS Utrophin GFP*. MO-mediated knockdown was performed as previously described (Herpers et al., 2008). CRISPR genome editing for *notch1b-15* was performed as described by Gagnon et al. (2014) using the primers listed in the supplementary Materials and Methods to generate $notch1b\text{-}15^{uq1mf}$ (203 bp deletion) allele.

The F_2 $notch1b\text{-}15^{uq1mf/uq1mf}$ was generated by in-crossing $notch1b\text{-}15^{uq1mf/+}$, while F_3 $notch1b\text{-}15^{uq1mf/uq1mf}$ was generated from the F_2 $notch1b\text{-}15^{uq1mf/uq1mf}$ in-cross, both in the *tg(flt1:YFP;lyve1:dsRed)* background.

Chromatin immunoprecipitation (ChIP)

Positive *tg(fli1a:Gal4FF;10×UAS:Sox18Ragged-mCherry)* fish larvae were collected at 26-28 hpf and processed as described in supplementary Materials and Methods (Mohammed et al., 2013). DNA amplification was performed using the TruSeq ChIP-seq Kit (Illumina, IP-202-1012) following immunoprecipitation. The library was quantified using the KAPA library quantification kit for Illumina sequencing platforms (KAPA Biosystems, KK4824) and 50 bp single-end reads were sequenced on a HiSeq 2500 (Illumina) following the manufacturer's protocol. FASTQ files were mapped to GRCz10/danRer10 genome assembly using bowtie (Langmead, 2010), and peaks were called using MACS version 2.1.0. using input as a reference. To avoid false-positive peaks calling due to the mCherry epitope, ChIP-seq with the mCherry epitope only was performed in parallel to SOX18Ragged-mCherry ChIP-seq and peaks called in these experimental conditions were subtracted from the peaks called in the SOX18Ragged-mCherry conditions. For details, see the supplementary Materials and Methods.

Motif identification and EMSA

Sequences were analysed for consensus sequence motifs by eye and using TRANSFAC (BIOBASE; http://genexplain.com/transfac/) (Matys et al., 2006). EMSAs were performed as previously described (De Val et al., 2004), as outlined in the supplementary Materials and Methods.

Morpholinos and drug treatment

MO-mediated knockdown was performed as previously described (Duong et al., 2014; Cermenati et al., 2008). ATG MOs against *sox7* and *sox18* were injected into the *tg(notch1b-15:GFP)* stable line at the 1-2 cell stage at 5 ng/embryo (Herpers et al., 2008). To assess the effect of *sox7/18* knockdown on endogenous *notch1b* transcripts, *sox7* and *sox18* MOs were injected into WT zebrafish larvae at 1 ng/embryo in parallel with a standard control MO (std-MO) injected at 2 ng/embryo (Cermenati et al., 2008). To characterise $notch1b\text{-}15^{uq1mf}$, *notch1b* MO was injected into the $notch1b\text{-}15^{uq1mf/+}$ cross at 5 ng/embryo. For MO sequences, see the supplementary Materials and Methods.

N-[(3,5-difluorophenyl)acetyl]-L-alanyl-2-phenyl]glycine-1,1-dimethylethyl ester (DAPT; Sigma-Aldrich) was used at 5 µM dissolved in 1% DMSO. Fish were treated from the 15- to 16-somite stage to 3 dpf and the medium containing DAPT was refreshed daily.

In situ hybridisation and immunofluorescence staining

Whole-mount *in situ* hybridisation in zebrafish larvae was performed as described (Coxam et al., 2015; Duong et al., 2014). Section and whole-mount *in situ* hybridisation in mouse was performed as described (Metzis et al., 2013; Fowles et al., 2003). The *Notch1* probe was generated by PCR from mouse embryo cDNA pool at E14.5, and reverse transcribed with T7 polymerase. Whole-mount immunohistochemistry for anti-GFP was performed as described (Koltowska et al., 2015). For details, see the supplementary Materials and Methods.

Quantification and data analysis

To characterise the vasculature in Fig. 8E-G and Figs S6, S7, intersomitic vessels (20-22 ISVs) expressing *tg(flt1:YFP)* were analysed across 10-11 somites through a *z*-stack using ImageJ (NIH) after image acquisition by confocal microscopy. Intersomitic vessels connecting the dorsal longitudinal anastomotic vessel to the dorsal aorta expressing YFP were assigned as arterial ISVs. Vessels were also scored for ectopic sprouting. The proportion of aISVs or hypersprouts among the total number of ISVs was analysed by two-tailed Mann–Whitney *U*-test. To quantify the GFP intensity of *tg(notch1b-15:GFP)* and *tg(notch1b-15mutSOX-a/b:GFP)* (Fig. 7A), two to three ISVs across five to six somites in the trunk region were analysed using ImageJ. A region of interest (ROI) covering a single ISV was selected and mean pixel intensity for each ISV was quantified from each individual stack across three *z*-sections. This value was further corrected by subtracting the background value. Average ISV GFP intensity (quantified from two to three ISVs) for each fish larva was subsequently corrected for its genomic *GFP* copy number. A similar method was used to quantify GFP intensity in the endothelial lining along the dorsal aorta.

Fluorescence-activated cell sorting (FACS) and expression analysis

Flt1:YFP-positive endothelial cells were isolated from WT and F_3 $notch1b\text{-}15^{uq1mf/uq1mf}$ at 24-28 hpf. RNA was extracted, amplified and cDNA was synthesized as previously described (Coxam et al., 2014; Picelli et al., 2014). Primer sequences and details of the quantitative PCR analysis are provided in the supplementary Materials and Methods.

Acknowledgements

We thank M. Shipman for help with imaging. The ZED vector was kindly provided by F. Tessadori (Bakkers lab, Hubrecht Institute). The *notch1b* plasmid used to generate the probe was kindly provided by N. D. Lawson (University of Massachusetts Medical School).

Competing interests

The authors declare no competing or financial interests.

Author contributions

Conceptualization: I.K.-N.C., M.Frit., S.D.V., M.Fran.; Methodology: I.K.-N.C., M.Frit., S.D.V., M.Fran.; Formal analysis: K.H., J.C.; Investigation: I.K.-N.C., M.Frit., C.P.-T., A.N., K.H., A.L., J.O., D.D., A.O., D.H., E.L., K.L., I.R., M.C., B.H.; Resources: A.L., G.B.-G., J.C., S.S.-M., M.B.; Data curation: K.H., J.C.; Writing - original draft: I.K.-N.C., S.D.V., M.Fran.; Writing - review & editing: I.K.-N.C., B.H., M.B., S.D.V., M.Fran.; Visualization: I.K.-N.C., S.D.V., M.Fran.; Supervision: G.B.-G., J.C., E.D., B.H., M.B., S.D.V., M.Fran.; Project administration: S.D.V., M.Fran.; Funding acquisition: S.D.V., M.B., M.Fran.

Funding

This work was supported by the National Health and Medical Research Council of Australia (NHMRC) (APP1107643); The Cancer Council Queensland (1107631) (M.Fran.); the Australian Research Council Discovery Project (DP140100485) and a Career Development Fellowship (APP1111169) (M.Fran.); the Ludwig Institute for Cancer Research (M.Frit., A.N., I.R., S.D.V.); the Medical Research Council (MR/J007765/1) (K.L., G.B.-G., S.D.V.); the Fondazione Cariplo (2011-0555) (M.B., B.H., M.Fran.); and the Biotechnology and Biological Sciences Research Council (BB/L020238/1) (A.N., K.L., G.B.-G., S.D.V.). Deposited in PMC for release after 6 months.

Data availability

ChIP-seq data are available in the ArrayExpress database at EMBL-EBI (www.ebi.ac.uk/arrayexpress) with accession number E-MTAB-5843.

Supplementary information

Supplementary information available online at
http://dev.biologists.org/lookup/doi/10.1242/dev.146241.supplemental

References

Abdelilah, S., Mountcastle-Shah, E., Harvey, M., Solnica-Krezel, L., Schier, A. F., Stemple, D. L., Malicki, J., Neuhauss, S. C., Zwartkruis, F., Stainier, D. Y. et al. (1996). Mutations affecting neural survival in the zebrafish Danio rerio. *Development* **123**, 217-227.

Becker, P. W., Sacilotto, N., Nornes, S., Neal, A., Thomas, M. O., Liu, K., Preece, C., Ratnayaka, I., Davies, B., Bou-Gharios, G. et al. (2016). An intronic Flk1 enhancer directs arterial-specific expression via RBPJ-mediated venous repression. *Arterioscler. Thromb. Vasc. Biol.* **36**, 1209-1219.

Bessa, J., Tena, J. J., de la Calle-Mustienes, E., Fernández-Miñán, A., Naranjo, S., Fernández, A., Montoliu, L., Akalin, A., Lenhard, B., Casares, F. et al. (2009). Zebrafish enhancer detection (ZED) vector: a new tool to facilitate transgenesis and the functional analysis of cis-regulatory regions in zebrafish. *Dev. Dyn.* **238**, 2409-2417.

Bogdanović, O., Fernández-Miñán, A., Tena, J. J., de la Calle-Mustienes, E., Hidalgo, C., van Kruysbergen, I., van Heeringen, S. J., Veenstra, G. J. C. and Gómez-Skarmeta, J. L. (2012). Dynamics of enhancer chromatin signatures mark the transition from pluripotency to cell specification during embryogenesis. *Genome Res.* **22**, 2043-2053.

Bray, S. J. (2006). Notch signalling: a simple pathway becomes complex. *Nat. Rev. Mol. Cell Biol.* **7**, 678-689.

Bussmann, J., Bos, F. L., Urasaki, A., Kawakami, K., Duckers, H. J. and Schulte-Merker, S. (2010). Arteries provide essential guidance cues for lymphatic endothelial cells in the zebrafish trunk. *Development* **137**, 2653-2657.

Cannavò, E., Khoueiry, P., Garfield, D. A., Geeleher, P., Zichner, T., Gustafson, E. H., Ciglar, L., Korbel, J. O. and Furlong, E. E. M. (2016). Shadow enhancers are pervasive features of developmental regulatory networks. *Curr. Biol.* **26**, 38-51.

Carmeliet, P., Ferreira, V., Breier, G., Pollefeyt, S., Kieckens, L., Gertsenstein, M., Fahrig, M., Vandenhoeck, A., Harpal, K., Eberhardt, C. et al. (1996). Abnormal blood vessel development and lethality in embryos lacking a single VEGF allele. *Nature* **380**, 435-439.

Cermenati, S., Moleri, S., Cimbro, S., Corti, P., Del Giacco, L., Amodeo, R., Dejana, E., Koopman, P., Cotelli, F. and Beltrame, M. (2008). Sox18 and Sox7 play redundant roles in vascular development. *Blood* **111**, 2657-2666.

Chong, D. C., Koo, Y., Xu, K., Fu, S. and Cleaver, O. (2011). Stepwise arteriovenous fate acquisition during mammalian vasculogenesis. *Dev. Dyn.* **240**, 2153-2165.

Corada, M., Orsenigo, F., Morini, M. F., Pitulescu, M. E., Bhat, G., Nyqvist, D., Breviario, F., Conti, V., Briot, A., Iruela-Arispe, M. L. et al. (2013). Sox17 is indispensable for acquisition and maintenance of arterial identity. *Nat. Commun.* **4**, 2609.

Coxam, B., Sabine, A., Bower, N. I., Smith, K. A., Pichol-Thievend, C., Skoczylas, R., Astin, J. W., Frampton, E., Jaquet, M., Crosier, P. S. et al. (2014). Pkd1 regulates lymphatic vascular morphogenesis during development. *Cell Rep.* **7**, 623-633.

Coxam, B., Neyt, C., Grassini, D. R., Le Guen, L., Smith, K. A., Schulte-Merker, S. and Hogan, B. M. (2015). carbamoyl-phosphate synthetase 2, aspartate transcarbamylase, and dihydroorotase (cad) regulates Notch signaling and vascular development in zebrafish. *Dev. Dyn.* **244**, 1-9.

De Val, S. and Black, B. L. (2009). Transcriptional control of endothelial cell development. *Dev. Cell* **16**, 180-195.

De Val, S., Anderson, J. P., Heidt, A. B., Khiem, D., Xu, S.-M. and Black, B. L. (2004). Mef2c is activated directly by Ets transcription factors through an evolutionarily conserved endothelial cell-specific enhancer. *Dev. Biol.* **275**, 424-434.

Duarte, A., Hirashima, M., Benedito, R., Trindade, A., Diniz, P., Bekman, E., Costa, L., Henrique, D. and Rossant, J. (2004). Dosage-sensitive requirement for mouse Dll4 in artery development. *Genes Dev.* **18**, 2474-2478.

Duong, T., Koltowska, K., Pichol-Thievend, C., Le Guen, L., Fontaine, F., Smith, K. A., Truong, V., Skoczylas, R., Stacker, S. A., Achen, M. G. et al. (2014). VEGFD regulates blood vascular development by modulating SOX18 activity. *Blood* **123**, 1102-1112.

Fowles, L. F., Bennetts, J. S., Berkman, J. L., Williams, E., Koopman, P., Teasdale, R. D. and Wicking, C. (2003). Genomic screen for genes involved in mammalian craniofacial development. *Genesis* **35**, 73-87.

François, M., Caprini, A., Hosking, B., Orsenigo, F., Wilhelm, D., Browne, C., Paavonen, K., Karnezis, T., Shayan, R., Downes, M. et al. (2008). Sox18 induces development of the lymphatic vasculature in mice. *Nature* **456**, 643-647.

Francois, M., Koopman, P. and Beltrame, M. (2010). SoxF genes: Key players in the development of the cardio-vascular system. *Int. J. Biochem. Cell Biol.* **42**, 445-448.

Gagnon, J. A., Valen, E., Thyme, S. B., Huang, P., Akhmetova, L. Pauli, A., Montague, T. G., Zimmerman, S., Richter, C. and Schier, A. F. (2014). Efficient mutagenesis by Cas9 protein-mediated oligonucleotide insertion and large-scale assessment of single-guide RNAs. *PLoS ONE* **9**, e98186.

Gale, N. W., Dominguez, M. G., Noguera, I., Pan, L., Hughes, V., Valenzuela, D. M., Murphy, A. J., Adams, N. C., Lin, H. C., Holash, J. et al. (2004). Haploinsufficiency of delta-like 4 ligand results in embryonic lethality due to major defects in arterial and vascular development. *Proc. Natl. Acad. Sci. USA* **101**, 15949-15954.

Geudens, I., Herpers, R., Hermans, K., Segura, I., Ruiz de Almodovar, C., Bussmann, J., De Smet, F., Vandevelde, W., Hogan, B. M., Siekmann, A. et al. (2010). Role of delta-like-4/Notch in the formation and wiring of the lymphatic network in zebrafish. *Arterioscler. Thromb. Vasc. Biol.* **30**, 1695-1702.

Gore, A. V., Monzo, K., Cha, Y. R., Pan, W. and Weinstein, B. M. (2012). Vascular development in the zebrafish. *Cold Spring Harb. Perspect. Med.* **2**, a006684-a006684.

Harvey, S. A., Sealy, I., Kettleborough, R., Fényes, F., White, R., Stemple, D. and Smith, J. C. (2013). Identification of the zebrafish maternal and paternal transcriptomes. *Development* **140**, 2703-2710.

Heintzman, N. D. and Ren, B. (2009). Finding distal regulatory elements in the human genome. *Curr. Opin. Genet. Dev.* **19**, 541-549.

Hermkens, D. M. A., van Impel, A., Urasaki, A., Bussmann, J., Duckers, H. J. and Schulte-Merker, S. (2015). Sox7 controls arterial specification in conjunction with hey2 and efnb2 function. *Development* **142**, 1695-1704.

Herpers, R., van de Kamp, E., Duckers, H. J. and Schulte-Merker, S. (2008). Redundant roles for Sox7 and Sox18 in arteriovenous specification in zebrafish. *Circ. Res.* **102**, 12-15.

Hollenhorst, P. C., McIntosh, L. P. and Graves, B. J. (2011). Genomic and biochemical insights into the specificity of ETS transcription factors. *Annu. Rev. Biochem.* **80**, 437-471.

Hosking, B., François, M., Wilhelm, D., Orsenigo, F., Caprini, A., Svingen, T., Tutt, D., Davidson, T., Browne, C., Dejana, E. et al. (2009). Sox7 and Sox17 are strain-specific modifiers of the lymphangiogenic defects caused by Sox18 dysfunction in mice. *Development* **136**, 2385-2391.

Jahnsen, E. D., Trindade, A., Zaun, H. C., Lehoux, S., Duarte, A. and Jones, E. A. V. (2015). Notch1 is pan-endothelial at the onset of flow and regulated by flow. *PLoS ONE* **10**.

James, K., Hosking, B., Gardner, J., Muscat, G. E. and Koopman, P. (2003). Sox18 mutations in the ragged mouse alleles ragged-like and opossum. *Genesis* **36**, 1-6.

Kent, W. J., Sugnet, C. W., Furey, T. S., Roskin, K. M., Pringle, T. H., Zahler, A. M. and Haussler, D. (2002). The human genome browser at UCSC. *Genome Res.* **12**, 996-1006.

Kim, K., Kim, I.-K., Yang, J. M., Lee, E., Koh, B. I., Song, S., Park, J., Lee, S., Choi, C., Kim, J. W. et al. (2016). SoxF transcription factors are positive feedback regulators of VEGF signaling. *Circ. Res.* **119**, 839-852.

Koltowska, K., Paterson, S., Bower, N. I., Baillie, G. J., Lagendijk, A. K., Astin, J. W., Chen, H., François, M., Crosier, P. S., Taft, R. J. et al. (2015). mafba is a downstream transcriptional effector of Vegfc signaling essential for embryonic lymphangiogenesis in zebrafish. *Genes Dev.* **29**, 1618-1630.

Krebs, L. T., Xue, Y., Norton, C. R., Shutter, J. R., Maguire, M., Sundberg, J. P., Gallahan, D., Closson, V., Kitajewski, J., Callahan, R. et al. (2000). Notch signaling is essential for vascular morphogenesis in mice. *Genes Dev.* **14**, 1343-1352.

Krebs, L. T., Shutter, J. R., Tanigaki, K., Honjo, T., Stark, K. L. and Gridley, T. (2004). Haploinsufficient lethality and formation of arteriovenous malformations in Notch pathway mutants. *Genes Dev.* **18**, 2469-2473.

Kwan, K. M., Fujimoto, E., Grabher, C., Mangum, B. D., Hardy, M. E., Campbell, D. S., Parant, J. M., Yost, H. J., Kanki, J. P. and Chien, C. B. (2007). The Tol2kit: a multisite gateway-based construction kit for Tol2 transposon transgenesis constructs. *Dev. Dyn.* **236**, 3088-3099.

Lanahan, A. A., Hermans, K., Claes, F., Kerley-Hamilton, J. S., Zhuang, Z. W., Giordano, F. J., Carmeliet, P. and Simons, M. (2010). VEGF receptor 2 endocytic trafficking regulates arterial morphogenesis. *Dev. Cell* **18**, 713-724.

Langmead, B. (2010). Aligning short sequencing reads with Bowtie. *Curr. Protoc. Bioinformatics* **11**, 11.7.

Lathen, C., Zhang, Y., Chow, J., Singh, M., Lin, G., Nigam, V., Ashraf, Y. A., Yuan, J. X., Robbins, I. M. and Thistlethwaite, P. A. (2014). ERG-APLNR axis controls pulmonary venule endothelial proliferation in pulmonary Veno-occlusive disease. *Circulation* **130**, 1179-1191.

Lawson, N. D. (2003). phospholipase C gamma-1 is required downstream of vascular endothelial growth factor during arterial development. *Genes Dev.* **17**, 1346-1351.

Lawson, N. D., Scheer, N., Pham, V. N., Kim, C. H., Chitnis, A. B., Campos-Ortega, J. A. and Weinstein, B. M. (2001). Notch signaling is required for arterial-venous differentiation during embryonic vascular development. *Development* **128**, 3675-3683.

Lawson, N. D., Vogel, A. M. and Weinstein, B. M. (2002). sonic hedgehog and vascular endothelial growth factor act upstream of the Notch pathway during arterial endothelial differentiation. *Dev. Cell* **3**, 127-136.

Lee, S.-H., Lee, S., Yang, H., Song, S., Kim, K., Saunders, T. L., Yoon, J. K., Koh, G. Y. and Kim, I. (2014). Notch pathway targets proangiogenic regulator Sox17 to restrict angiogenesis. *Circ. Res.* **115**, 215-226.

Liu, Z.-J., Shirakawa, T., Li, Y., Soma, A., Oka, M., Dotto, G. P., Fairman, R. M., Velazquez, O. C. and Herlyn, M. (2003). Regulation of Notch1 and Dll4 by vascular endothelial growth factor in arterial endothelial cells: implications for modulating arteriogenesis and angiogenesis. *Mol. Cell. Biol.* **23**, 14-25.

Lizama, C. O., Hawkins, J. S., Schmitt, C. E., Bos, F. L., Zape, J. P., Cautivo, K. M., Borges Pinto, H., Rhyner, A. M., Yu, H., Donohoe, M. E. et al. (2015). Repression of arterial genes in hemogenic endothelium is sufficient for haematopoietic fate acquisition. *Nat. Commun.* **6**, 7739.

Matys, V., Kel-Margoulis, O. V., Fricke, E., Liebich, I., Land, S., Barre-Dirrie, A., Reuter, I., Chekmenev, D., Krull, M., Hornischer, K. et al. (2006). TRANSFAC and its module TRANSCompel: transcriptional gene regulation in eukaryotes. *Nucleic Acids Res.* **34**, D108-D110.

Mertin, S., McDowall, S. G. and Harley, V. R. (1999). The DNA-binding specificity of SOX9 and other SOX proteins. *Nucleic Acids Res.* **27**, 1359-1364.

Metzis, V., Courtney, A. D., Kerr, M. C., Ferguson, C., Rondon Galeano, M. C., Parton, R. G., Wainwright, B. J. and Wicking, C. (2013). Patched1 is required in neural crest cells for the prevention of orofacial clefts. *Hum. Mol. Genet.* **22**, 5026-5035.

Mohammed, H., D'Santos, C., Serandour, A. A., Ali, H. R., Brown, G. D., Atkins, A., Rueda, O. M., Holmes, K. A., Theodorou, V., Robinson, J. L. L. et al. (2013). Endogenous purification reveals GREB1 as a key estrogen receptor regulatory factor. *Cell Rep.* **3**, 342-349.

Pendeville, H., Winandy, M., Manfroid, I., Nivelles, O., Motte, P., Pasque, V., Peers, B., Struman, I., Martial, J. A. and Voz, M. L. (2008). Zebrafish Sox7 and Sox18 function together to control arterial-venous identity. *Dev. Biol.* **317**, 405-416.

Pennisi, D., Bowles, J., Nagy, A., Muscat, G. and Koopman, P. (2000a). Mice null for Sox18 are viable and display a mild coat defect. *Mol. Cell. Biol.* **20**, 9331-9336.

Pennisi, D., Gardner, J., Chambers, D., Hosking, B., Peters, J., Muscat, G., Abbott, C. and Koopman, P. (2000b). Mutations in Sox18 underlie cardiovascular and hair follicle defects in ragged mice. *Nat. Genet.* **24**, 434-437.

Phng, L.-K. and Gerhardt, H. (2009). Angiogenesis: a team effort coordinated by notch. *Dev. Cell* **16**, 196-208.

Picelli, S., Faridani, O. R., Björklund, A. K., Winberg, G., Sagasser, S. and Sandberg, R. (2014). Full-length RNA-seq from single cells using Smart-seq2. *Nat. Protoc.* **9**, 171-181.

Quillien, A., Moore, J. C., Shin, M., Siekmann, A. F., Smith, T., Pan, L., Moens, C. B., Parsons, M. J. and Lawson, N. D. (2014). Distinct Notch signaling outputs pattern the developing arterial system. *Development* **141**, 1544-1552.

Robinson, A. S., Materna, S. C., Barnes, R. M., De Val, S., Xu, S.-M. and Black, B. L. (2014). An arterial-specific enhancer of the human endothelin converting enzyme 1 (ECE1) gene is synergistically activated by Sox17, FoxC2, and Etv2. *Dev. Biol.* **395**, 379-389.

Roca, C. and Adams, R. H. (2007). Regulation of vascular morphogenesis by Notch signaling. *Genes Dev.* **21**, 2511-2524.

Sabo, P. J., Hawrylycz, M., Wallace, J. C., Humbert, R., Yu, M., Shafer, A., Kawamoto, J., Hall, R., Mack, J., Dorschner, M. O. et al. (2004). Discovery of functional noncoding elements by digital analysis of chromatin structure. *Proc. Natl. Acad. Sci. USA* **101**, 16837-16842.

Sacilotto, N., Monteiro, R., Fritzsche, M., Becker, P. W., Sanchez-del-Campo, L., Liu, K., Pinheiro, P., Ratnayaka, I., Davies, B., Goding, C. R. et al. (2013). Analysis of Dll4 regulation reveals a combinatorial role for Sox and Notch in arterial development. *Proc. Natl. Acad. Sci. USA* **110**, 11893-11898.

Sakamoto, Y., Hara, K., Kanai-Azuma, M., Matsui, T., Miura, Y., Tsunekawa, N., Kurohmaru, M., Saijoh, Y., Koopman, P. and Kanai, Y. (2007). Redundant roles of Sox17 and Sox18 in early cardiovascular development of mouse embryos. *Biochem. Biophys. Res. Commun.* **360**, 539-544.

Siekmann, A. F. and Lawson, N. D. (2007). Notch signalling limits angiogenic cell behaviour in developing zebrafish arteries. *Nature* **445**, 781-784.

Visconti, R. P., Richardson, C. D. and Sato, T. N. (2002). Orchestration of angiogenesis and arteriovenous contribution by angiopoietins and vascular endothelial growth factor (VEGF). *Proc. Natl. Acad. Sci. USA* **99**, 8219-8224.

Wong, E. S., Thybert, D., Schmitt, B. M., Stefflova, K., Odom, D. T. and Flicek, P. (2015). Decoupling of evolutionary changes in transcription factor binding and gene expression in mammals. *Genome Res.* **25**, 167-178.

Wu, J., Iwata, F., Grass, J. A., Osborne, C. S., Elnitski, L., Fraser, P., Ohneda, O., Yamamoto, M. and Bresnick, E. H. (2005). Molecular determinants of NOTCH4 transcription in vascular endothelium. *Mol. Cell. Biol.* **25**, 1458-1474.

Wythe, J. D., Dang, L. T. H., Devine, W. P., Boudreau, E., Artap, S. T., He, D., Schachterle, W., Stainier, D. Y. R., Oettgen, P., Black, B. L. et al. (2013). ETS factors regulate Vegf-dependent arterial specification. *Dev. Cell* **26**, 45-58.

Zhou, Y., Williams, J., Smallwood, P. M. and Nathans, J. (2015). Sox7, Sox17, and Sox18 cooperatively regulate vascular development in the mouse retina. *PLoS ONE* **10**, e0143650.

Zhou, P., Gu, F., Zhang, L., Akerberg, B. N., Ma, Q., Li, K., He, A., Lin, Z., Stevens, S. M., Zhou, B. et al. (2017). Mapping cell type-specific transcriptional enhancers using high affinity, lineage-specific Ep300 bioChIP-seq. *eLife* **6**, e22039.

Supplemental Materials and Methods

Detailed Methods

Cloning

The 10XUAS:Sox18Ragged-mCherry plasmid DNA was generated using the full-length mouse *Sox18Ragged* cDNA sequence cloned into the Gateway pME vector (pDON-221) using Gateway technology (Hartley et al., 2000). Subsequently a Gateway LR reaction was performed combining a p5E-10xUAS, pME-Sox18Ragged and p3E-mcherry placing the final 10xUAS:Sox18Ragged-mCherry sequence into pDestTol2CG2. The *notch1b- 15:GFP* construct was generated by PCR from zebrafish genomic DNA using the primers described below, cloned via the Gateway pME vector (pDON-221) into the Zebrafish Enhancer Detector (ZED) vector (Bessa et al., 2009). The *notch1b- 15mutSOX-a/b* sequence was generated by site-directed PCR mutagenesis using the primers listed below, and cloned as described for the WT construct.

The *NOTCH1-68*, *NOTCH1+3/5*, and *NOTCH1+33* enhancers were generated by PCR from mouse genomic DNA using primers listed below. PCR products were cloned into the pCR8 vector using the pCR8/GW/TOPO TA Cloning Kit (Invitrogen, K2500-20) following manufacturer's instructions.

The *NOTCH1+16* WT and *NOTCH1+16mutSOX-a/b* enhancers were initially generated as custom-made, double-stranded linear DNA fragments (GeneArt® Strings™, Life Technologies). Sequences are provided below. These fragments were subsequently cloned into the pCR8 vector using the pCR8/GW/TOPO TA Cloning Kit as described for PCR fragments . Once cloning was confirmed, the enhancer sequence was transferred from the pCR8/GW/enhancer entry vector to the hsp68-LacZ-Gateway vector (provided by N. Ahituv) using Gateway LR Clonase II Enzyme mix (Life Technologies, 11791-100) following manufacturer's instructions.

Primer sequences

NOTCH1-68 WT: F-cctgggcaacagagcaagac; R-ccagggtctgtgcaactttgc

NOTCH1+3/5 WT: F-gagctgtcatcgctgcattattg: R-cgcctttgggctctctgtttg

NOTCH1+33 WT: F-caaacaagggctgcgatggag; R-gatgcaggtgaatccttagcag

notch1b-15-WT (gateway homology arm underlined):

F-ggggacaagtttgtacaaaaaagcaggctctgtgggatctgcttggtgt;

R-ggggaccactttgtacaagaaagctgggtagctaactgcgcgaactgga

notch1b-15mutSOX-a (mutated site underlined): F-

cagttcccttacggcaaaaaaaatttggctgcataat;

R-attatgcagccaaatttttttgccgtaagggaactg

notch1b-15mutSOX-b (mutated site underlined): F-

gaggtacttcccccctaaaaaatgttggaggttgtgtg;

R-cacacaacctccaacatttttttaggggaagtacctc

Linear DNA fragment sequences

Human *NOTCH1+16* WT- cacagcgcagggacccagccggggtctgagccggggccaggctttccggcc
caaacagctgttgccggcacccccagctcttttgtctgcaaatcttttcccccagttgcatcctcggatggtttaaaatgtgc
gaaggaggaagtgcaggaaggccaggtttcctcctctggctccggggaaacccttttgtgtgggaggcgggatgggg
acagaacctgtcctcccgggaagctacctttcccgcagccgggaaaacaatgccctcacccgac
Human *NOTCH1+16* mutSOXa/b (mutated site underlined)-
cacagcgcagggacccagccggggtctgagccggggccaggct
ttccggcccaaacagctgttgccggcacccccagctcttttgtctgcaaatcttttcccccagttgcatcctcggatggttta
aaatgtgcgaaggaggaagtgcaggaaggccaggtttcctcctctggctccggggaaaccctgcctgtgggaggcg
ggatggggacagaacctgtcctcccgggaagctacctttcccgcagccgggaaggcagtgccctcacccgac

Generation and analysis of transgenic and mutant mice

Where appropriate, animal procedures were approved by local ethical review and licensed by the UK Home Office, or conformed to institutional guidelines (University of Queensland Animal Ethics Committee). Transgenic mice were generated by oocyte microinjection as described previously (De Val et al., 2004). Transgenic mouse embryos were collected along with yolk sac and placenta at the indicated time-point after breeding. Embryos were dissected away from uterine horn, separated from placenta and yolk sac, rinsed in ice-cold 1 X PBS and fixed in 2% PFA, 0.2% glutaraldehyde, 1 X PBS at 4°C. Embryos at embyonic stage (E) 8 were fixed for 10 minutes, E9 embryos were fixed for 30 minutes, E11 and E12 embryos were fixed for 60 minutes, whereas E15 samples were fixed for 120 minutes. After fixation, embryos were incubated for 60 mins in rinse solution (0.1% sodium deoxycholate, 0.2% Nonidet P-40, 2 mmol/L MgCl2, 1 X PBS) at 4°C. After fixation and rinse, embryos were stained overnight at room temperature in 1 mg/ml 5-bromo-4-chloro-3-indolyo-β-D-galactoside solution (X-gal) containing 5 mmol/L potassium ferrocyanide, 5 mmol/L ferricyanide, 0.1% sodium deoxycholate, 0.2% Nonidet P-40, 2 mmol/L MgCl2 and 1 X PBS. After staining, embryos were rinsed through a series of 1 X PBS washes, then fixed overnight in 4% paraformaldehyde at 4°C. E15 embryos were cleared using a protocol adapted from (Schatz et al., 2005). Fixed and X-Gal stained embryos were rinsed in water and were then incubated in a series of clearing solutions consisting of glycerol and 1% (w/v) KOH. The glycerol ratio of the solutions was increased in steps from 20% to 50%, 80%, and finally 100% glycerol. Specimens were incubated in each solution for 4 days at 37°C and, after the transparency seemed sufficient, imaged submerged in 100% glycerol under a stereomicroscope.

Imaging of whole embryos and organs was performed using a stereo microscope (Leica M165C) equipped with a ProGres CF Scan camera (Jenoptik) and ProgRes CapturePro software (Jenoptik). For each enhancer, embryos were also sectioned for histological analysis to investigate X-gal staining patterns. For histological analysis, embryos were dehydrated through a series of ethanol washes, cleared by xylene and paraffin wax-embedded. 5 or 6-µm sections were prepared, de-waxed, and

counterstained with nuclear fast red (Electron Microscopy Sciences). Staining for Endomucin was performed on de-waxed sections from previously X-gal stained embryos using a dilution of 1:100 rat anti-Endomucin antibody (Santa Cruz, sc-65495) in PBS as described previously (Sacilotto et al., 2013).

The placenta was used for genotyping. Tissue samples were incubated over-night at 55°C with 500µL GNT buffer (50mmol/L KCl, 1.5mmol/L MgCl2, 10mmol/L Tris-pH8, 0.01% gelatin, 0.45% nonidet P40, 0.45% Tween) and proteinase K (10mg/ml). Afterwards, the solution was heated to 95°C for 30 minutes and centrifuged for 1 minute at maximum rpm in a benchtop centrifuge. 0.5µL of this supernatant were subsequently used in a PCR reaction with the GoTag Green master mix (Promega, M7122) using LacZ PCR primer F- gttgcagtgcacggcagatacacttgctga and R-gccactggtgtgggccataattcaattcgc.

Compound *Sox7*$^{-/-}$;*Sox18*$^{-/-}$ (C57BL/6) mouse embryos were generated on the C57BL/6 background through crossing heterozygous *Sox7:tm1* (C57BL/6) to *Sox18:tm1* (C57BL/6), generating *Sox7*$^{+/-}$;*Sox18*$^{+/-}$ mice which were subsequently in-crossed (Pennisi et al., 2000). Genotype was confirmed by PCR using the following primers: *mSox7*(F)- TGTAACTTGGAGATCCATAGAGC, *mSox7(*R)-TCATTCTCAGTATTGTTT TGCC, *mSox7lacZ*(R)-TGGATCAGCTAAGCCAGGT, *mSox18*(F)-CCCGACGTCCATCAG ACCTC*, mSox18*(R)-GTCGCTTGCGCTCGTCCTTC, *mSox18lacZ*(R)CGCCCGTTGCACC ACAGATG
All animals used were 7-24 weeks old.

Generation and analysis of transgenic and mutant zebrafish
Mosaic transgenic zebrafish embryos were generated using the Tol2 system in conjunction with the ZED vector (Bessa et al., 2009). Briefly, 1nL of reaction mix containing Tol2 and ZED *notch1b-15*:GFP at a final concentration of 30ng/µl (stable line) and 50ng/µl (transient analysis) was injected into 1 cell wild type embryos. The *tg(notch1b-15:GFP)* stable line was created by outcrossing the F0 adult carriers generated using the Tol2 system. The *sox7*^{hu5626};*sox18*^{hu10320} double homozygous mutant zebrafish are as previously described (Hermkens et al., 2015). The *tg*(*fli1a:Gal4FF;UAS:Sox18Ragged-mCherry)* zebrafish line was generated by crossing *10XUAS:Sox18Ragged-mCherry* with *fli1a:Gal4FF*, *4XUAS Utrophin GFP*.

Generation of *sox7*$^{-/-}$;*sox18*$^{-/-}$ null zebrafish was as previously described (Hermkens et al., 2015). Morpholino used were:
sox7-MO1 (zfin:MO1-so7): 5'-CGCACTTATCAGAGCCGCCATGTGC-3'
sox18-MO1(zfin: MO1-sox18): 5'-ATATTCATTCCAGCAAGACCAACAC-3'
sox7-MO2 (zfin: MO5-sox7): 5'-ACGCACTTATCAGAGCCGCCATGTG – 3'
sox18-MO2 (zfin: MO5-sox18): 5'-TATTCATTCCAGCAAGACCAACACG -3′
notch1b-MO (zfin MO2-notch1b) 5'-AATCTCAAACTGACCTCAAACCGAC-3'

To introduce genomic modification into the *notch1b-15* locus in zebrafish, two guide RNAs were generated according to a published protocol (Gagnon et al., 2014) using the following primers:

notch1b-15-CRISPRgRNA1: 5'-GCTCTATCTCTGCACAATGCTGG-3'

notch1b-15-CRISPRgRNA2: 5'-GAAGAGAAATGGGGCGACGTGGG-3'

1nl of *notch1b-15* gRNA1 and gRNA2 were injected into 1-2 cell wild-type zebrafish embryo at a final concentration of 100ng/µl together with Cas9 RNA (150ng/µl) in one injection mix. To rapidly screen for potential modification on the targeted allele, single embryo DNA extraction and High Resolution Melting Analysis (HRMA) was performed as previously described (Dahlem et al., 2012) using the primers below:

notch1b-15-gRNA1-HRMA: F-GTCTGTTTTTGGAGAGTCCACAGC and R-CTACAGCTCTGCGGTGCATTG
*notch1b-15*gRNA2-HRMA: F-GTACTTCCCCCTTTTGTTTGTTG and R-TTCGCGGATTGGTGAGAATGAA -3'

notch1b-15 ^{uq1mf} was genotyped by PCR using:
notch1b15^{uq1mf}*_seq* F-GAGAGTCCACAGCTGCTTCCC and R-GAAATGCATTCGCGGATTGGT

Chromatin immunoprecipitation sequencing (ChIP) experiments, libraries and analysis

Positive *tg(fli1a:Gal4FF;10XUAS:Sox18Ragged-mCherry)* fish larvae (based on GFP expression in the heart) were collected at 26-28hpf, fixed in 1% formaldehyde for 10 mins, and quenched with 1 mol/L glycine. Fish were dissociated with a mortar and pestle in liquid nitrogen, lysed and subsequent immunoprecipitation was performed using DsRed polyclonal antibody (Clontech, #632496). The remaining of the sample preparation was performed as previously described in (Mohammed et al., 2013).

DNA amplification was performed using 0.5 µmol/L of the universal reverse PCR primer and forward PCR primer containing the index sequence of choice in 50 µL 1 x NEBNext High-Fidelity PCR Master Mix (New England Biolabs, M0541). The number of PCR cycles ranged from 13 to 18, depending on the ChIP efficiency. The PCR product was purified using AMPure beads (1.8 volume) and eluted in 20 µL of resuspension buffer (Tris-Acetate 10 mmol/L pH 8).

EMSA

Electrophoretic mobility shift assay (EMSAs) were performed as described previously (De Val et al., 2004). Proteins were made using the TNT Quick Coupled Transcription/Translation system as described in the manufacturer's directions. The full length mouse Sox7 and Sox18 were in the pCITE2 plasmid, and transcribed using T7 polymerase. Etv2 was in the pCS2 plasmid, and transcribed using Sp6 polymerase. Double stranded oligonucleotides were labeled with 32P-dCTP to create a DNA probe, using Klenow (Promega) to fill in overhanging 5' ends. This probe was subsequently purified on a non-denaturing 8% polyacrylamide-TBE gel. Each lane contained 20 µl binding reaction, consisting of protein or lysate control (5 µl Sox7 and Sox18, 1 µl Etv2) and 2 µl 10X binding buffer (40mmol/L KCl, 15 mmol/L HEPES pH 7.9, 1 mmol/L EDTA, 0.5 mmol/L DTT, 5% glycerol). For Etv2, 0.5 µg of poly dI-dC was used. For Sox7 and Sox18, 0.25µg poly-dG-dC was used. For competitor lanes, a 100-fold excess of competitor DNA was added in a volume of 1µl. Binding reactions were incubated at room temperature for 20 minutes before the addition of radiolabeled probed, after which they were incubated an additional 20-40 minutes. Gels were electrophoresed on a 6% non-denaturing polyacrylamide gel at 4°C.

Fluorescent Activated Cell sorting (FACS)

FltYFP positive endothelial cells were isolated from WT and *notch1b-15*$^{uq1mf/1mf}$ at 48hpf. RNA was extracted, amplified and cDNA was synthesized as previously described (Coxam et al., 2014; Dahlem et al., 2012; De Val et al., 2004; Mohammed et al., 2013; Picelli et al., 2014).

Quantitative PCR

For GFP copy number quantification in *tg(notch1b-15)* and *tg*(*notch1b-15mutSOX-a/b:GFP)* larvae, quantitative PCR was performed on genomic DNA with the following primers:

GFP-qpcr: F-CAGAAGAACGGCATCAAGGTG; R-GGACTGGGTGCTCAGGTAGTG

Genomic control1-qPCR: F- GAGCAGGAACTGAGGGAAGC; R-TCTCCACAACTTCCAGTCCG

Genomic control2-qPCR: F-ATGTCTTAAAAGCCCTCCCGGT; R-AGGTTGCTGGTAGTCCATACTGTT

To quantify the transcript level from sorted Flt+ cells, the following primers were used:

notch1b-qpcr: F-CAAACGATCACTAGACGGCT; R-ATCGATCTCACTTGTGACGG

notch1a-qpcr: F-GCCCGGATGGTCAGGTAAAA; R-TGTAGTGCGACTCAAACGCT

notch3-qpcr: F-TGACCCTAATGGCTATCGGT; R-CACACAGGTGCCCTGATTTA

her6-qpcr: F-GCGTACTTGACAGCGTTTAC; R-TAGAAGACTTTCTGTGTTCCGA

kdrl-qpcr: F-CTTGACCAGGGTGGATAACG; R-CGATTGATCCGCTCCTTATG

flt1-qpcr: F- TCCTCTCCACCGGATAACTC; R-TCGGCTTCTTGATATGCGTT

dll4-qpcr: F-ATTATTGAGGCCTGGCACTC; R- CAGACAGATCGGTTCTTCGC

hey1-qpcr: F-CAAGCAAGAAAACGTCGCAG; R- GTGCAGTCTCTGCTAGACATT

hey2-qpcr: F- TGGGCAGCGAGAATAACTAC; R- TTTTCAATGATCCCTCTCCGC

sox18-qpcr: F- CGCTGTGCTCAGTAAAATGC; R- ACGCTTGTCGAGTGTGCTC

notch2-qpcr: F-TGTATGCCAGGCTTTGATGGA; R-AGGACACTCGCAGACGAATC

In situ hybridization, immunofluorescence staining and imaging

Wholemount *in situ* hybridization in zebrafish larvae was performed as previously described (Coxam et al., 2015). Probes used were *notch1b*, *flt1* and *cdh5* (provided by N. D. Lawson) and *egfp* (Duong et al., 2014). Wholemount and section mouse *in situ* was performed as described in (Metzis et al., 2013; Fowles et al., 2003). The *Notch1* probe was generated with the following primers from mouse embryo cDNA pool at 14.5dpc, and reverse transcribed with T7 polymerase.

For wholemount mouse *in situ*:
*mNotch1*_1-ISH: F-CACACCCCTCATGATTGCCT; R (T7 promoter=underlined)-CGATGTTAATACGACTCACTATAGGGGTCCAGCAACACTTTGGCAG

For section mouse *in situ*:
*mNotch1*_2-ISH: F-TGAGAATGATGCCCGCACTT; R (T7 promoter=underlined) -CGATGTTAATACGACTCACTATAGGGACATTGCCGGTTGTCGATCT

Wholemount immunohistochemistry for anti-GFP was performed as described previously (Koltowska et al., 2015). Antibody used was anti-GFP (1:300, Abcam, #ab13970) and goat anti-chicken IgG Alexa 488 (1:300, Invitrogen, A11039) and DAPI (1:1000, Sigma Aldrich).

Live and fixed embryos were mounted laterally in 1% low-melting agarose and imaged using a Zeiss LSM 710 FCS confocal microscope (Zeiss, Germany). Zebrafish embryos transgenic for either the *notch1b-15* WT:GFP or *notch1b-15mutSOX-a/b:GFP* constructs were generated in parallel and assessed for reporter gene expression. For transient analysis, expression of the GFP reporter gene in endothelial cells was assessed by confocal microscopy at 2dpf, using expression of the cardiac actin promoter (CAR):RFP internal control within the ZED vector to normalize for the variation of transgene expression associated with tol2-mediated mosaic transgenesis (Bessa et al., 2009). For mouse work, images were taken with a Leica MZFLIII epifluorescence stereomicroscope equipped with a DFC 480-R2 digital camera and the LAS imaging software (Leica, Germany). Images were processed using the Adobe Photoshop, Adobe Illustrator software (Adobe, CA) and ImageJ (NIH Image, USA).

Supplemental Figures

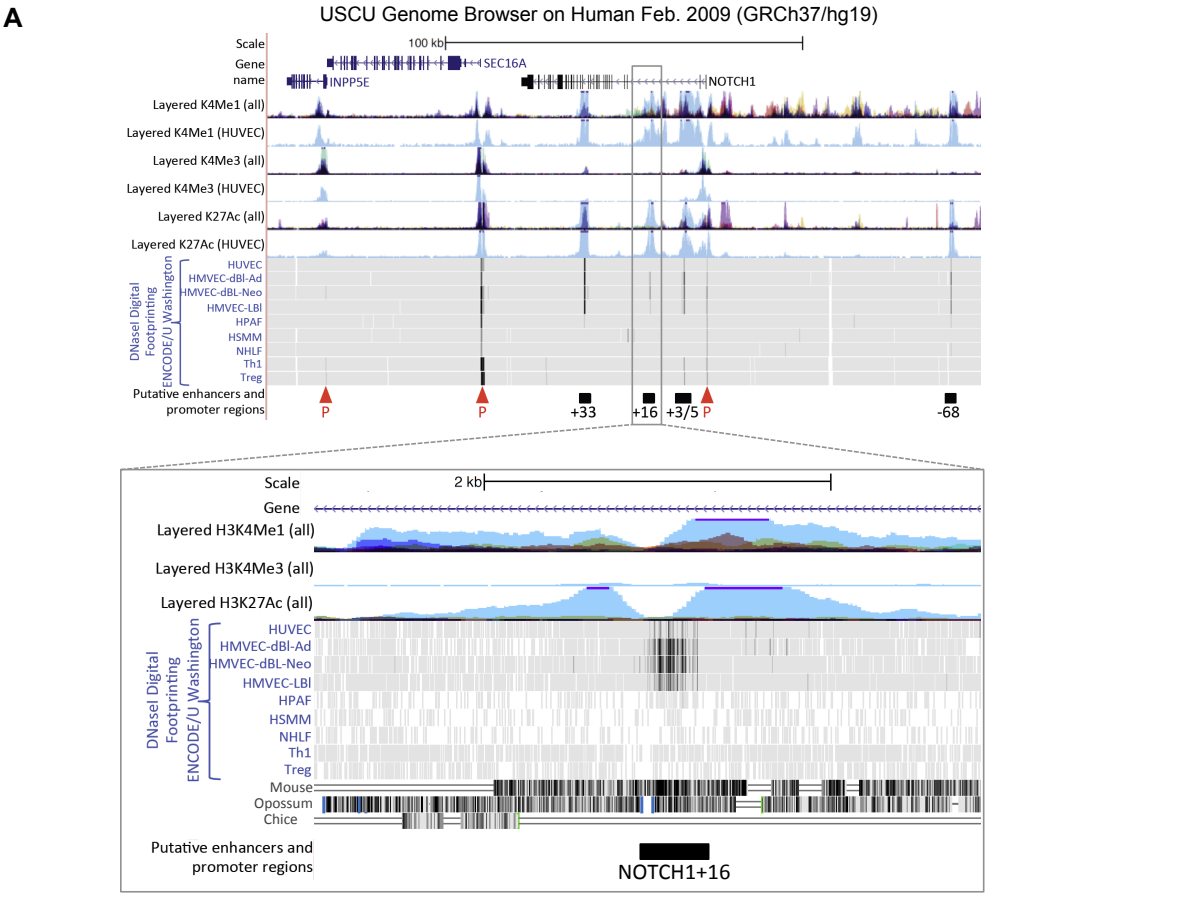

Supplemental Figure 1

Supplemental Figure 1. Analysis of the *NOTCH1+16* enhancer region.

(A) Schematic representation of the 3kb region framing the *NOTCH1+16* enhancer within the human *NOTCH1* locus from UCSC ENCODE Browser http://genome.ucsc.edu. HUVEC specific H3Me1 and H3K27Ac (enhancer associated) and H3K4Me3 (promoter associated) peaks are denoted in light blue (combined tracks, denoted as 'all'), other colors indicate H3K4Me1, H3K4Me3 and H3K4Ac peaks specific to non-endothelial cell lines (GM12878 cells (red), H1-hESC cells (yellow), HSMM cells (green), K562 cells (purple) NHEK cells (lilac) and NHLF cells (pink)). DNase I digital hypersensitive hotspots are indicated by black vertical lines on grey (HUVEC, HMVEC-dBl-Ad, HMVEC-dBl-Neo and HMVEC-LBl, all different endothelial cell types). The *NOTCH1+16* putative enhancer region was identified by high levels of HUVEC-specific H3K4Me1 and H3K27Ac associated with endothelial cell-specific DNaseI hypersensitivity hotspots. Bottom of figure, black parallel lines indicate detected conservation between species.

(B) Screen shot from ECR Browser (http://ecrbrowser.dcode.org) showing significant levels of conservation across multiple species for the *NOTCH1+16* enhancer (orange coloured peaks). Analysis used default parameters for conservation, although no additional species conservation was captured by lowering the threshold.

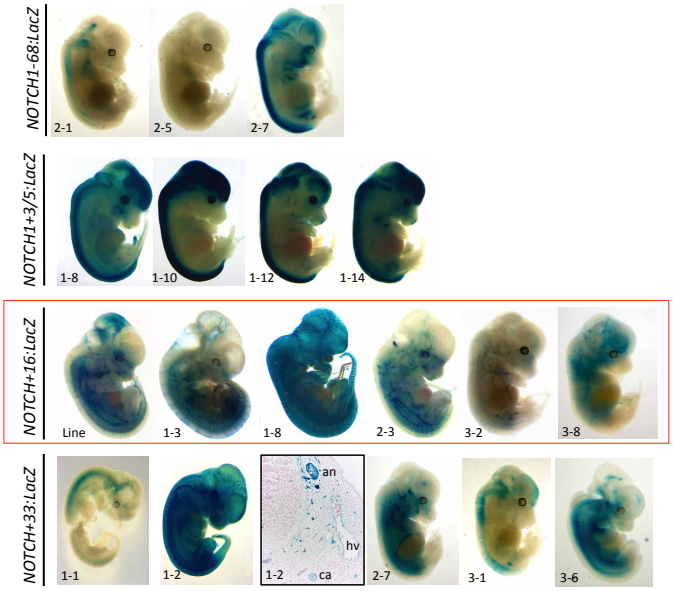

Supplemental Figure 2

Supplemental Figure 2. Analysis of the *NOTCH1* locus identified four putative enhancer elements.

Whole-mount *lacZ* staining for E12-E13 transient transgenic embryos with *Notch1* putative enhancers. Numbers on bottom left of each picture indicate unique embryo identifier. Section on bottom row (black box) demonstrates the pan-vascular staining pattern detected in the one vascular-positive *Notch1+33:LacZ* embryo #1-2. an = accessory nerve, ca =carotid artery, hv =head vein.

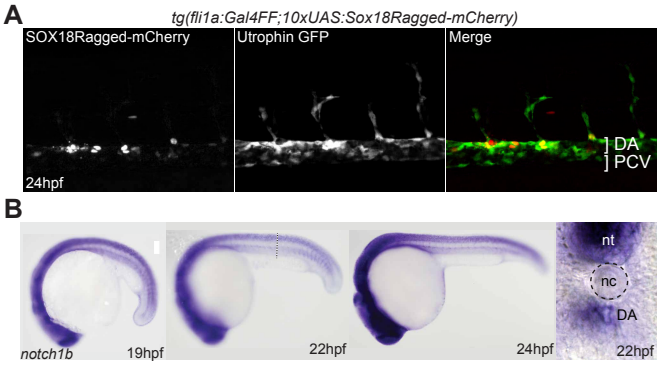

Supplemental Figure 3. Expression of Sox18Ragged-mcherry and endogenous *notch1b* in developing zebrafish larvae.
(A) The *tg(fli1a:Gal4FF;10XUAS:Sox18Ragged-mcherry)* line used to perform Sox18Ragged ChIP-Seq experiments. mCherry-Sox- 18Ragged fusion protein (red) could be observed in trunk blood vasculature (green).
(B) *notch1b* mRNA is detected in arterial endothelial cells through-out embryonic development in a pattern similar to the *notch1b-15:GFP* transgene. nt = neural tube, nc = notochord, DA = dorsal aorta, PCV= posterior cardinal vein.

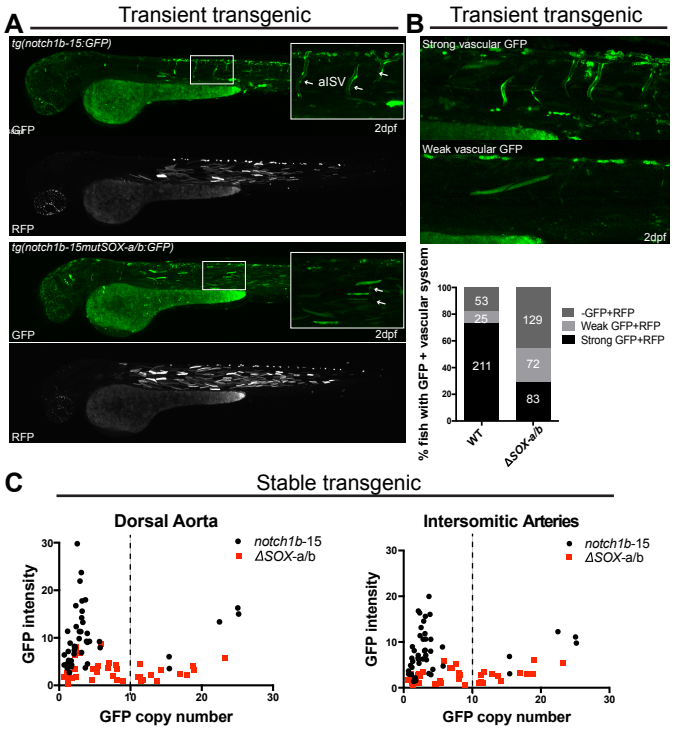

Supplemental Figure 4

Supplemental Figure 4. Sox sites ablation compromises *notch1b-15* enhancer activity.

(A) A representative confocal projection of wild-type zebrafish F_0 larvae injected with *notch1b-15:GFP* (top panel) and *notch1b-15:mutSOX-a/b:GFP* (bottom panel). Bright GFP expression could be observed in the intersomittic vessel and dorsal aorta of fish injected with the wild-type *notch1b-15* construct, whereas expression of GFP in fish injected with the mutant construct is almost completely absent from the arterial vascular network (white arrows). (B) Graph indicating levels of GFP expression in F_0 zebrafish transgenic for *notch1b-15:GFP* and *notch1b-15mutSOX-a/b:GFP* transgenes. All scored fish were also positive for the internal control *cardiac actin:RFP* (+RFP). Number of zebrafish examined for each conditions was indicated, expression was scored as no (-), weak or strong GFP. (C) Scatter plots representing the relationship between genomic GFP copy number and GFP intensity in endothelial lining of dorsal aorta (left panel) and intersomittic vessels (right panel) in stable *tg(notch1b-15)* and *tg(notch1b-15mutSOX-a/b:GFP*). Only larvae with GFP copy number <10 were included in the analysis for Fig. 7B-C. Scored *tg(notch1b-15)*, n=46; *tg(notch1b-15mutSOX-a/b:GFP*), n=42; larvae were each pooled from 4 independent founders.

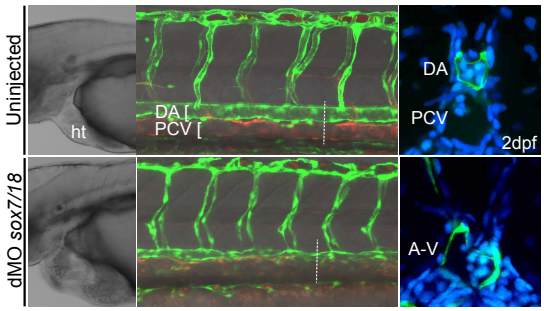

Supplemental Figure 5

Supplemental Figure 5. *sox7/18* morpholino characterization. *sox7/18* morpholino based knockdown of SoxF resulted in pericardial edema and fusion between the dorsal aorta and cardinal vein in zebrafish larvae. A-V = arterial venous shunts.

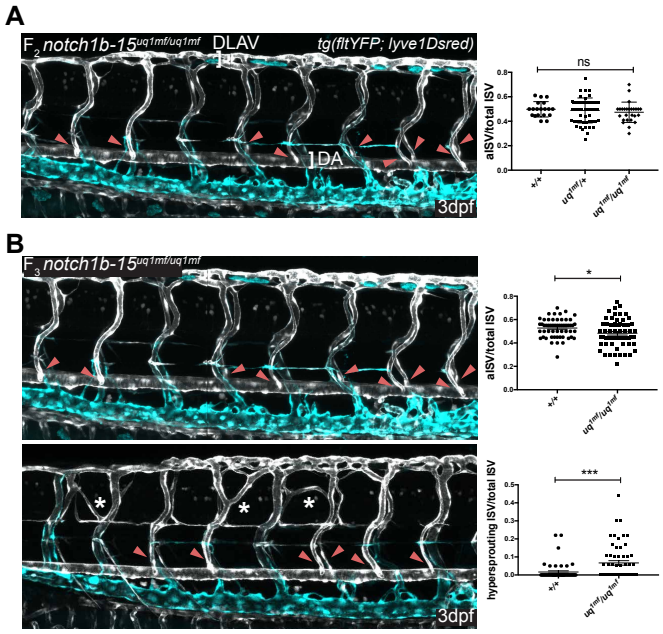

Supplemental Figure 6

Supplemental Figure 6. Loss of endogenous *notch1b-15* enhancer mildly phenocopies Notch1b loss-of-function.

(A) A representative confocal projection of F_2 homozygous zebrafish *notch1b-15*$^{uq1mf/uq1mf}$, derived from the F_1 heterozygous *notch1b-15*$^{uq1mf/+}$ in-crosses. No obvious phenotype was observed in the vasculature of F_2 homozygous clutches. Quantification of YFP positive intersomittic vessels connecting between the dorsal longitudinal anastomotic vessel (DLAV) and dorsal aorta (DA) in individual F_2 larvae labeled by *tg(fltYFP;lyveDsred)* at 3dpf (red arrowheads). Mean ± SEM; Scored sibling WT (*+/+*), n=19; Het (*uq*$^{1mf/+}$), n=54; Hom (*uq*$^{1mf/1mf}$), n=26; Mann-Whitney. (ns) No significant difference. (B) Representative confocal projections of F_3 homozygous zebrafish *notch1b-15*$^{uq1mf/uq1mf}$, derived from the F_2 homozygous *notch1b-15*$^{uq1mf/uq1mf}$ in-crosses. While most F_3 homozygous clutches lack phenotype (top left panel), a sub-population (20-30%) of the larvae showed either ectopic sprouting (asterisks) and/or loss of arterial connections (red arrowheads) between DLAV and DA, as indicated by the loss of YFP expression in *tg(fltYFP;lyve1Dsred)* background (bottom left panel). Quantification of YFP positive (top right panel) and hyper-sprouting (bottom right panel) intersomitic vessels in individual F_3 larvae labeled by *tg(fltYFP;lyveDsred)* at 3dpf. Mean ± SEM; Scored WT (*+/+*), n=55; Hom (*uq*$^{1mf/1mf}$), n=59; Mann-Whitney. (*) p<0.05, (***) p<0.001.

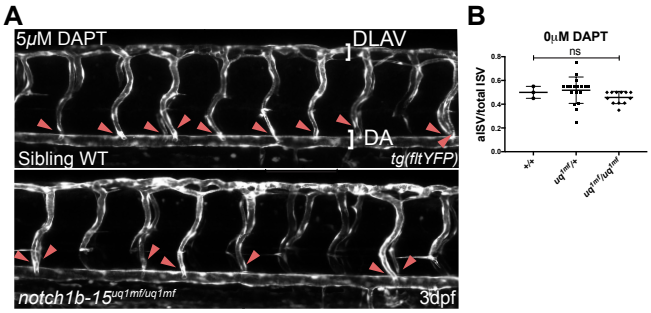

Supplemental Figure 7

Supplemental Figure 7. Partial Notch inhibition results in the loss of arterial identity in *notch1b-15* endogenous mutant fish.

(A) At 3dpf, *notch1b-15*$^{uq1mf/uq1mf}$ mutant embryos treated with 5μM DAPT showed a significant reduction in the number of arterial connections (red arrowheads) between the dorsal longitudinal anastomotic vessel (DLAV) and dorsal aorta (DA), as indicated by the loss of YFP expression in the *tg(fltYFP)* background. (B) Quantification of YFP positive intersomitic vessels that connect between DLAV and DA in control (0μM DAPT) individual embryos at 3dpf. Vessels are labeled by *tg(fltYFP)*. Mean ± SEM; scored sibling WT (*+/+*), n=3; Het (*uq*$^{1mf/+}$), n=18; Hom (*uq*$^{1mf/1mf}$), n=12; Mann-Whitney. (ns) No significant difference.

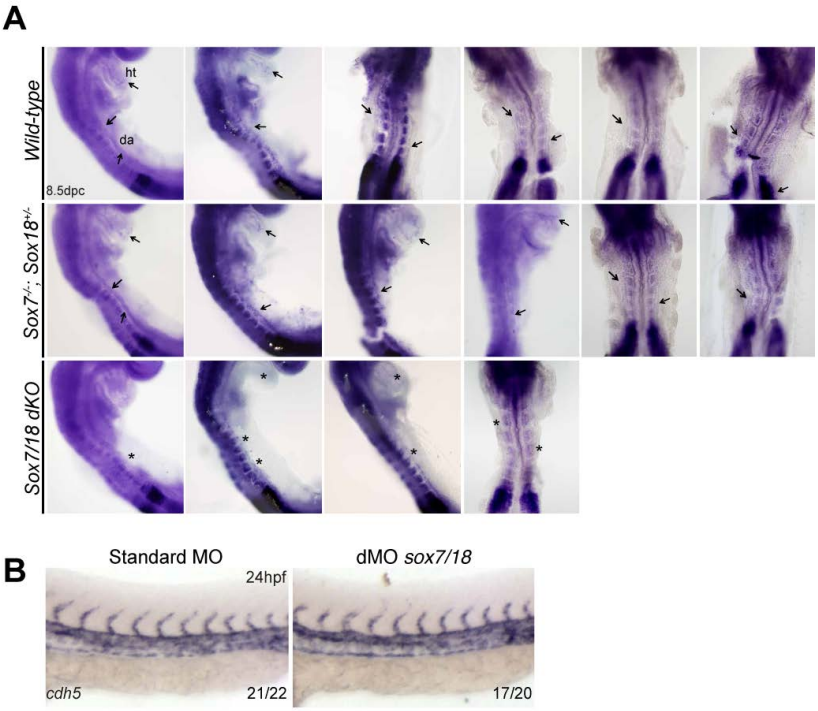

Supplemental Figure 8

Supplemental Figure 8. Expression profiling of SOX7/18 mutant mice and zebrafish mophants.

(A) Wholemount *in situ* hybridization assay showed a reduction of *Notch1* expression in the primitive heart cavity and dorsal aorta (asterisks) in *Sox7/Sox18* double knock-outs at 8.5dpc (8-11ss) compared to the WT control and *Sox7*$^{-/-}$*; Sox18*$^{+/-}$ control (black arrows). ht = heart, da = dorsal aorta.

(B) Wholemount *in situ* hybirdization showed a comparable *cdh5* expresison between control and *sox7/18* double morphants, indicating that vascular structures were correctly formed in these morphants.

References

Bessa, J., Tena, J. J., La Calle-Mustienes, De, E., Fernández-Miñán, A., Naranjo, S., Fernández, A., Montoliu, L., Akalin, A., Lenhard, B., Casares, F., et al. (2009). Zebrafish enhancer detection (ZED) vector: a new tool to facilitate transgenesis and the functional analysis of cis-regulatory regions in zebrafish. *Dev Dyn* **238**, 2409–2417.

Coxam, B., Neyt, C., Grassini, D. R., Le Guen, L., Smith, K. A., Schulte-Merker, S. and Hogan, B. M. (2015). carbamoyl-phosphate synthetase 2, aspartate transcarbamylase, and dihydroorotase (cad) regulates Notch signaling and vascular development in zebrafish. *Dev Dyn* **244**, 1–9.

Coxam, B., Sabine, A., Bower, N. I., Smith, K. A., Pichol-Thievend, C., Skoczylas, R., Astin, J. W., Frampton, E., Jaquet, M., Crosier, P. S., et al. (2014). Pkd1 regulates lymphatic vascular morphogenesis during development. *Cell Rep* **7**, 623–633.

Dahlem, T. J., Hoshijima, K., Jurynec, M. J., Gunther, D., Starker, C. G., Locke, A. S., Weis, A. M., Voytas, D. F. and Grunwald, D. J. (2012). Simple methods for generating and detecting locus-specific mutations induced with TALENs in the zebrafish genome. *PLoS Genet* **8**, e1002861.

De Val, S., Anderson, J. P., Heidt, A. B., Khiem, D., Xu, S.-M. and Black, B. L. (2004). Mef2c is activated directly by Ets transcription factors through an evolutionarily conserved endothelial cell-specific enhancer. *Dev Biol* **275**, 424–434.

Duong, T., Koltowska, K., Pichol-Thievend, C., Le Guen, L., Fontaine, F., Smith, K. A., Truong, V., Skoczylas, R., Stacker, S. A., Achen, M. G., et al. (2014). VEGFD regulates blood vascular development by modulating SOX18 activity. *Blood* **123**, 1102–1112.

Fowles, L. F., Bennetts, J. S., Berkman, J. L., Williams, E., Koopman, P., Teasdale, R. D. and Wicking, C. (2003). Genomic screen for genes involved in mammalian craniofacial development. *Genesis* **35**, 73–87.

Hartley, J. L., Temple, G. F. and Brasch, M. A. (2000). DNA Cloning Using In Vitro Site-Specific Recombination. *Genome Res* **10**, 1788–1795.

Hermkens, D. M. A., van Impel, A., Urasaki, A., Bussmann, J., Duckers, H. J. and Schulte-Merker, S. (2015). Sox7 controls arterial specification in conjunction with hey2 and efnb2 function. *Development* **142**, 1695–1704.

Gagnon, J.A., Valen E., Thyme, S.B., Huang, P., Akhmetova, L., Pauli, A., Montague, T.G., Zimmerman, S., Richter, C. and Schier, A.F. (2014). Efficient mutagenesis by Cas9 protein-mediated oligonucleotide insertion and large-scale assessment of single-guide RNAs. *PLoS ONE* **9**, e98186

Koltowska, K., Paterson, S., Bower, N. I., Baillie, G. J., Lagendijk, A. K., Astin, J. W., Chen, H., François, M., Crosier, P. S., Taft, R. J., et al. (2015). mafba is a downstream transcriptional effector of Vegfc signaling essential for embryonic lymphangiogenesis in zebrafish. *Genes Dev*.

Metzis, V., Courtney, A. D., Kerr, M. C., Ferguson, C., Rondon Galeano, M. C., Parton, R. G., Wainwright, B. J. and Wicking, C. (2013). Patched1 is required in neural crest cells for the prevention of orofacial clefts. *Hum Mol Genet* **22**, 5026–5035.

Mohammed, H., D'Santos, C., Serandour, A. A., Ali, H. R., Brown, G. D., Atkins, A., Rueda, O. M., Holmes, K. A., Theodorou, V., Robinson, J. L. L., et al. (2013). Endogenous Purification Reveals GREB1 as a Key Estrogen Receptor Regulatory Factor. *Cell Rep* **3**, 342–349.

Pennisi, D., Bowles, J., Nagy, A., Muscat, G. and Koopman, P. (2000). Mice Null for Sox18 Are Viable and Display a Mild Coat Defect. *Mol Cell Biol* **20**, 9331–9336.

Picelli, S., Faridani, O. R., Björklund, A. K., Winberg, G., Sagasser, S. and Sandberg, R. (2014). Full-length RNA-seq from single cells using Smart-seq2. *Nat Protoc* **9**, 171–181.

Sacilotto, N., Monteiro, R., Fritzsche, M., Becker, P. W., Sanchez-del-Campo, L., Liu, K., Pinheiro, P., Ratnayaka, I., Davies, B., Goding, C. R., et al. (2013). Analysis of Dll4 regulation reveals a combinatorial role for Sox and Notch in arterial development. *Proc Natl Acad Sci USA* **110**, 11893–11898.

Schatz, O., Golenser, E. and Ben-Arie, N. (2005). Clearing and photography of whole mount X-gal stained mouse embryos. *BioTechniques* **39**, 650–652– 654 passim.